Biogeosciences

# Bottom-water deoxygenation at the Peruvian margin during the last deglaciation recorded by benthic foraminifera

Zeynep Erdem[1], Joachim Schönfeld[2], Anthony E. Rathburn[3], Maria-Elena Pérez[4], Jorge Cardich[5], and Nicolaas Glock[2]

[1]NIOZ Royal Netherlands Institute for Sea Research, and Utrecht University,
P.O. Box 59, 1790 AB Den Burg, Texel, the Netherlands
[2]GEOMAR Helmholtz Centre for Ocean Research Kiel, Wischhofstr. 1–3, 24148 Kiel, Germany
[3]Department of Geological Sciences, California State University, Bakersfield, CA 93311, USA
[4]Department of Palaeontology, Natural History Museum, London, UK
[5]Instituto del Mar del Peru (IMARPE), A. Gamarra y Gral. Valle, Chucuito, Callao 01, Peru

**Correspondence:** Zeynep Erdem (zeynep.erdem@nioz.nl)

**Abstract.** Deciphering the dynamics of dissolved oxygen in the mid-depth ocean during the last deglaciation is essential to understand the influence of climate change on modern oxygen minimum zones (OMZs). Many paleo-proxy records from the eastern Pacific Ocean indicate an extension of oxygen-depleted conditions during the deglaciation, but the degree of deoxygenation has not been quantified to date. The Peruvian OMZ, one of the largest OMZs in the world, is a key area to monitor such changes in near-bottom-water oxygenation in relation to changing climatic conditions. Here, we analysed the potential to use the composition of foraminiferal assemblages from the Peruvian OMZ as a quantitative redox proxy. A multiple regression analysis was applied to a joint dataset of living (rose-bengal-stained, fossilizable calcareous species) benthic foraminiferal distributions from the Peruvian continental margin. Bottom-water oxygen concentrations ($[O_2]_{BW}$) during sampling were used as the dependant variable. The correlation was significant ($R^2 = 0.82$; $p < 0.05$), indicating that the foraminiferal assemblages are rather governed by oxygen availability than by the deposition of particulate organic matter ($R^2 = 0.53$; $p = 0.31$). We applied the regression formula to three sediment cores from the northern part of the Peruvian OMZ between 3 and 8° S and 997 and 1250 m water depth, thereby recording oxygenation changes at the lower boundary of the Peruvian OMZ. Each core displayed a similar trend of decreasing oxygen levels since the Last Glacial Maximum (LGM). The overall $[O_2]_{BW}$ change from the LGM and the Holocene was constrained to 30 µmol kg$^{-1}$ at the lower boundary of the OMZ.

## 1 Introduction

Oxygen minimum zones (OMZs) occur where intense upwelling and high primary productivity result in elevated oxygen consumption within the water column in combination with sluggish ventilation (Wyrtki, 1962; Helly and Levin, 2004; Fuenzalida et al., 2009). In today's world oceans, the most pronounced OMZs with oxygen concentrations $<20$ µmol kg$^{-1}$ are observed offshore of northwest and southwest Africa, in the Arabian Sea and Bay of Bengal in the Indian Ocean, and along the continental margin of the eastern Pacific at low latitudes (Helly and Levin, 2004; Paulmier and Ruiz-Pino, 2009). Warmer conditions have contributed to expansion of OMZs during the last decades (Stramma et al., 2008; Schmidtko et al., 2017; Levin, 2018; Oschlies et al., 2018). Paleoceanographic reconstructions of bottom-water oxygenation during the last deglaciation are a valuable approach to understand the dynamics of OMZs during changing climatic conditions (e.g. Jaccard and Galbraith, 2012; Moffitt et al., 2015; Praetorius et al., 2015). The eastern equatorial Pacific (EEP) has been the focus of various paleoceanographic studies to unravel the dynamics of surface productivity and bottom-water oxygenation (Oberhänsli

et al., 1990; Heinze and Wefer, 1992; Cannariato and Kennett, 1999; Loubere, 1999; Hendy and Pedersen, 2006; Martinez and Robinson, 2010; Moffitt et al., 2014; Scholz et al., 2014; Salvatteci et al., 2016; Tetard et al., 2017; Balestra et al., 2018; Hoogakker et al., 2018; Cardich et al., 2019). The region is characterized by a strong and shallow OMZ maintained as a result of persistent upwelling (Pennington et al., 2006). Previous studies in the region used established paleoproxies such as sedimentary textures (laminations), productivity indicators ($C_{org}$, $\delta^{15}N$, biogenic opal), redox-sensitive elements (e.g. U, Mo, Cd, V, Mn) and benthic foraminiferal distributions (e.g. Jaccard et al., 2014; Moffitt et al., 2015). Most of the studies reported that cold glacial periods were generally associated with contracted OMZ, whereas warm or interglacial periods were associated with an expansion of the OMZ at intermediate depths. However, only a few studies attempted bottom-water oxygen reconstructions of the Peruvian margin, and they used records from sediment cores recovered from depths shallower than 400 m (Oberhänsli et al., 1990; Heinze and Wefer, 1992; Scholz et al., 2014; Moffitt et al., 2015; Salvatteci et al., 2016). In a review, Schönfeld et al. (2015) demonstrated that the deposition of laminated sediments indicated oxygen concentrations $<7\,\mu mol\,kg^{-1}$ and that accumulation rates of sedimentary organic carbon could be used to quantify oxygen concentrations of $>10\,\mu mol\,kg^{-1}$. A geochemical approach focusing on the Peruvian margin used redox-sensitive elements (Fe, Mo, U) and found a 5 to $10\,\mu mol\,kg^{-1}$ decrease from glacial to interglacial periods in the centre of the OMZ at depths between 100 and 500 m (Scholz et al., 2014). Because of the lack of complete records from the continental slope off Peru (Reimers and Suess, 1983; Erdem et al., 2016) and the limited applicability of some of the redox proxies (laminated sediments, Mo, U) at higher oxygen levels, paleo-oxygen reconstructions were not possible at the lower, dysoxic–oxic boundary of the Peruvian OMZ. However, benthic foraminiferal faunas were markedly structured with oxygenation at these depths (Mallon et al., 2012). Therefore, the present study aimed to reconstruct paleo-oxygen conditions since the Last Glacial Maximum (LGM) by using benthic foraminiferal records from sediment cores from the Peruvian OMZ between 900 and 1250 m water depth. We compiled all available information on living (rose-bengal-stained) benthic foraminiferal faunas from the Peruvian margin as a calibration dataset to investigate the following questions. (1) Did the Peruvian OMZ structure show differences in terms of vertical and horizontal extension since the LGM? (2) If there are such differences, can we actually quantify these changes in bottom-water oxygen concentrations ($[O_2]_{BW}$) by reverting to the oxygen demands of today's living faunas? (3) If so, how much did the $[O_2]_{BW}$ levels change since the LGM?

## 1.1 Benthic foraminifera as an oxygen proxy

Certain benthic foraminiferal species and assemblages have been suggested as proxies for bottom-water oxygenation, in particular for low-oxic to anoxic conditions (e.g. Sen Gupta and Machain-Castillo, 1993; Kaiho, 1994; Alve and Bernhard, 1995; Bernhard et al., 1997; Baas et al., 1998; Nordberg et al., 2000; Leiter and Altenbach, 2010). Since a high flux of particulate organic matter to the sea floor prevails in OMZs, these species also flourish under elevated food availability. Applications of certain species to reconstruct ancient bottom-water oxygen concentrations were often undermined by the TROX model (Barmawidjaja et al., 1992; Jorissen et al., 1995). This conceptual model explains the microhabitat structure of benthic foraminifera in the sediments as driven by the availability of both the organic matter and dissolved oxygen (Van der Zwaan, 1999). A growing number of publications reporting the living (rose-bengal-stained) benthic foraminiferal distributions and their ambient environmental conditions (Phleger and Soutar, 1973; Mackensen and Douglas, 1989; Sen Gupta and Machain-Castillo, 1993; Bernhard et al., 1997; den Dulk et al., 1998; Jannink et al., 1998; Levin et al., 2002; Schumacher et al., 2007; Cardich et al., 2012, 2015; Mallon et al., 2012; Caulle et al., 2014) showed some features in common. First, benthic foraminiferal faunas generally show a low diversity and high population density in oxygen-depleted environments; (2) most but not all living specimens in OMZs were found dwelling in the first 1 or 2 cm of the surface sediments here, even at moderate flux rates of particulate organic matter; (3) species with a thin, porous test wall (e.g. Bolivinids) always outnumber the agglutinated and porcelaneous species at low oxygen levels. Pore densities of the tests have been recognized as indicators of bottom- and pore-water redox conditions (Kaiho, 1994; Glock et al., 2011; Kuhnt et al., 2013; Rathburn et al., 2018). A comparison of different OMZ settings showed that benthic foraminiferal assemblages and distributions could be used to identify spatial changes of the OMZ provided certain threshold values and ranges are considered. However, the terminology, threshold values and units used in previous benthic foraminiferal studies were markedly different (Table 1). Here, we consider the following classification: microxic conditions $<5\,\mu mol\,kg^{-1}$, dysoxic conditions $5$–$45\,\mu mol\,kg^{-1}$ and oxic conditions $>45\,\mu mol\,kg^{-1}$. Overall, an extreme low-oxygen, even anoxia-tolerant association was found within the OMZ core, a transitional species group was recorded around the lower boundary of the OMZ ($>20\,\mu mol\,kg^{-1}$), and a cosmopolitan and much more diverse fauna was observed outside the OMZ (e.g. Table 2; Schumacher et al., 2007; Mallon et al., 2012; Caulle et al., 2014).

**Table 1.** Classification of different environments and thresholds of bottom-water dissolved oxygen ($[O_2]_{BW}$) for benthic foraminifera and benthic biota in general.

| Reference | $[O_2]_{BW}$ range (mL L$^{-1}$) | $[O_2]_{BW}$ range (µmol kg$^{-1}$) | Classification |
|---|---|---|---|
| Tyson and Pearson (1991) | 2–8 | 90–360 | oxic |
| Sen Gupta and Machain-Castillo (1993) | 0.2–2 | 9–90 | dysoxic |
| | 0–0.2 | 0–9 | suboxic |
| | 0 | 0 | anoxic |
| Kaiho (1994) | >1.5 | >67.5 | oxic |
| Baas et al. (1998) | 0.3–1.5 | 13.5–67.5 | suboxic |
| Cannariato et al. (1999) | 0.1–0.3 | 4.5–13.5 | dysoxic |
| | <0.1 | <4.5 | anoxic |
| Bernhard and Sen Gupta (1999) | >1 | >45 | oxic |
| Levin (2003) | 0.1–1 | 5–45 | dysoxic |
| Mallon et al. (2012) | <0.1 | <5 | microxic |
| Caulle et al. (2014) | 0 | 0 | anoxic |
| Rathburn et al. (2018) | >2 | >89 | oxic |
| | 0.5–2 | 22–89 | dysoxic |
| | <0.5 | <22 | suboxic |

## 1.2 Regional setting

The Peruvian OMZ is one of the most pronounced OMZs in the world (Fig. 1; Paulmier and Ruiz-Pino, 2009), covering the Peruvian continental shelf and upper slope, with its thickest part between 5 and 15° S and 50 and 750 m water depth (Fig. 2; Fuenzalida et al., 2009). The intensity of the OMZ is dependent on the low ventilation of advected intermediate waters, diapycnal mixing and the extremely high primary productivity in the surface waters (Karstensen et al., 2008; Brandt et al., 2015). The productivity is maintained by the wind-driven upwelling of cold, nutrient-rich and oxygen-poor waters from intermediate depths (e.g. Pennington et al., 2006). The main source of these upwelled waters is the Peru–Chile Undercurrent (PCUC). It originates around 3–5° S and flows southward between 50 and 300 m water depth (Montes et al., 2010; Chaigneau et al., 2013). The PCUC is fed by the equatorial undercurrent (EUC) and southern subsurface countercurrents (SSCCs; Montes et al., 2010). Below the PCUC, the northward-flowing Chile–Peru Deep Coastal Current (CPDCC) carries cold Antarctic Intermediate Waters as a thin layer (AAIW; Chaigneau et al., 2013).

## 2 Material and methods

### 2.1 Sediment cores

Three sediment cores were considered in this study (M77/2-50-4, 52-2 and 59-1). They were collected during expedition M77 leg 2 with R/V *Meteor* in 2008 from the continental slope between 3 and 9° S and water depths of 997 m and 1250 m around the lower boundary of today's OMZ (Figs. 1

and 2, Table 3). The age models of all cores were based on radiocarbon dating from the planktonic foraminiferal species *Neogloboquadrina dutertrei* which is supplemented with benthic oxygen isotope curves that were correlated to stacked standard records (Fig. 3; Stern and Lisiecki, 2014) and Antarctic ice cores (Members et al., 2006). The radiocarbon datings were performed at the Leibniz Laboratory for Radiometric Dating and Stable Isotope Research, University of Kiel (CAU) and by Beta Analytic Inc., Florida. For core M77/2-59-1, the data were reported by Mollier-Vogel et al. (2013) and for the other cores by Erdem et al. (2016). The radiocarbon ages were later calibrated applying the Marine13 marine calibration set (Reimer et al., 2013). Reservoir age corrections were done according to the marine database (http://calib.org/marine/, last access: 12 June 2020) ranging from 89 to 338 years (Erdem et al., 2016). The closest ^{14}C reservoir age records are from the equatorial Pacific (Zhao and Keigwin, 2018) and off Chile (Siani et al., 2013; Sarnthein et al., 2019), and they significantly differ from each other. The reservoir ages at our three study sites likely varied over the last deglaciation, and yet due to their regional proximity, they are not expected to be significantly different from each other. All ages are expressed in thousands of years (ka) before 1950 CE (abbreviated as cal ka). We focused on the following time intervals with 300- to 500-year resolution at each core: the late Holocene (LH; 3–5 cal ka), the early Holocene (EH; 8–10 cal ka), the Bølling Allerød/Antarctic Cold Reversal (BA/ACR; 13–14.5 cal ka), the Heinrich Stadial-1 (HS1; 15–17.5 cal ka), and the Last Glacial Maximum (LGM; 20–22 cal ka). For benthic foraminiferal analyses, 10–20 cm$^3$ sediment samples were wet sieved on a 63 µm screen immediately after they were taken, and the residues were dried at

**Table 2.** Common species considered in this study and reported from different oxygen-depleted environments.

| Species | Ecology |
| --- | --- |
| *Bolivina costata* | Characteristic species of the Peruvian margin, particularly on the shelf (Resig, 1981, 1990; Cardich et al., 2012); tolerant to low bottom-water oxygen $<5\,\mu\text{mol}\,\text{kg}^{-1}$ (Khusid, 1974; Resig, 1981; Mallon et al., 2012) even to sulfidic pore waters (Cardich et al., 2015); able to denitrify (Glock et al., 2019); used as a proxy for enhanced upwelling during interglacial periods (Heinze and Wefer, 1992). |
| *Bolivina seminuda* | Dominant in different OMZs (Phleger and Soutar, 1973; Hermelin and Shimmield, 1990; Bernhard et al., 1997; Ohga and Kitazato, 1997; Gooday et al., 2000; Cardich et al., 2012; Caulle et al., 2014); tolerant to extreme low oxygen $<2.5\,\mu\text{mol}\,\text{kg}^{-1}$ (Mallon, 2012; Cardich et al., 2015); able to use nitrate for respiration (Piña-Ochoa et al., 2010; Glock et al., 2019); better adapted to low oxygen levels compared to other *Bolivina* species, e.g. *B. spissa* (Glock et al., 2011); suggested as dysoxic indicator (Kaiho, 1994); used as a proxy for enhanced upwelling during interglacial periods (Heinze and Wefer, 1992) and for dysoxic conditions (Tetard et al., 2017). |
| *Bolivina spissa* | Common in the OMZs in the Pacific Ocean (Douglas and Heitman, 1979; Ingle et al., 1980; Mackensen and Douglas, 1989; Nomaki et al., 2006; Glud et al., 2009; Fontanier et al., 2014; Venturelli et al., 2018); indicates intermediate hypoxic conditions/lower boundary of the OMZ core (Mullins et al., 1985; Mallon, 2012); able to use nitrate for respiration (Glock et al., 2011, 2019); suggested as dysoxic indicator (Kaiho, 1994); used as a proxy for suboxic conditions (Cannariato and Kennett, 1999; Tetard et al., 2017), for intermediate hypoxia (Moffitt et al., 2014) and for bottom-water nitrate reconstruction (Glock et al., 2018). |
| *Bolivinita minuta* | Common in the OMZ of the Gulf of Panama (Golik and Phleger, 1977); mostly at the lower boundary/outside the core of the OMZ offshore of Peru–Chile (Ingle et al., 1980; Mallon, 2012). Other *Bolivinita* species are associated with sustained organic matter flux (Sarkar and Gupta, 2014, and the references therein). |
| *Bulimina exilis* | Dominant in different OMZs (Smith, 1964; Douglas and Heitman, 1979; Bernhard et al., 1997; den Dulk et al., 1998; Jannink et al., 1998; Caulle et al., 2014; Cardich et al., 2015); associated with fresh organic matter input (Caralp, 1989); suggested as dysoxic indicator (Kaiho, 1994); used as a proxy for dysoxic conditions (Cannariato and Kennett, 1999; Tetard et al., 2017) and severe hypoxia (McKay et al., 2015; Praetorius et al., 2015). |
| *Cassidulina delicata* | Common in the eastern Pacific OMZs at the lower continental slope (Uchio, 1960; Ingle et al., 1980) and under intermediate bottom-water oxygen concentrations, lowest observed is $4.5\,\mu\text{mol}\,\text{kg}^{-1}$ (Golik and Phleger, 1977; Douglas and Heitman, 1979; Resig, 1981; Mackensen and Douglas, 1989; Kaiho, 1994); used as a proxy for dysoxic conditions (Tetard et al., 2017). |
| *Epistominella exigua* | Cosmopolitan, typical in the deep-sea environment, opportunistic, associated with pulsed supply of phytodetritus (Gooday, 1988, 1993; Smart et al., 1994) and elevated bottom-water oxygen concentrations (Schmiedl et al., 1997; Jannink et al., 1998; Gupta and Thomas, 2003); reported as one of the dominant species along the Peru–Chile margin (Ingle et al., 1980; Resig, 1981). |
| *Epistominella pacifica* | Dominant offshore of Peru and California at dysoxic and suboxic conditions (Khusid, 1974; Douglas and Heitman, 1979; Mackensen and Douglas, 1989); suboxic to oxic conditions in the Gulf of Panama (Golik and Phleger, 1977). |
| *Hoeglundina elegans* | Reported as common in areas with variable organic matter input and elevated oxygen concentrations (Gooday, 2003, and the references therein; Sarkar and Gupta, 2014; Venturelli et al., 2018); also observed in dysoxic sediments (lowest oxygen values measured $9\,\mu\text{mol}\,\text{kg}^{-1}$; Douglas and Heitman, 1979; Mackensen and Douglas, 1989); indicator of elevated oxygenation (Schmiedl et al., 1997; Geslin et al., 2004). Aragonitic shell, prone to dissolution (Gonzales et al., 2017). |
| *Pyrgo murrhyna* | Suggested as oxic indicator (Kaiho, 1994); associated with low to moderate flux of organic matter and moderate bottom-water oxygen concentrations (Gooday, 2003; Sarkar and Gupta, 2014). Generally, large *Miliolids* are reported being restricted to higher oxygen concentrations (in Arabian Sea $>16\,\mu\text{mol}\,\text{kg}^{-1}$; Caulle et al., 2014) and suggested as a proxy for rapid ventilation of oxygen-depleted environments (den Dulk et al., 2000). |
| *Uvigerina peregrina* | Cosmopolitan (Gooday and Jorissen, 2012), associated with high organic matter input (Altenbach et al., 1999; Schönfeld and Altenbach, 2005); common in dysoxic sediments of different OMZs (Smith, 1964; Ingle et al., 1980; Ohga and Kitazato, 1997; Venturelli et al., 2018), particularly outside the OMZ core and at the OMZ lower boundary (Jannink et al., 1998; Mallon, 2012); used as a proxy for suboxic conditions (Cannariato and Kennett, 1999; Tetard et al., 2017). |
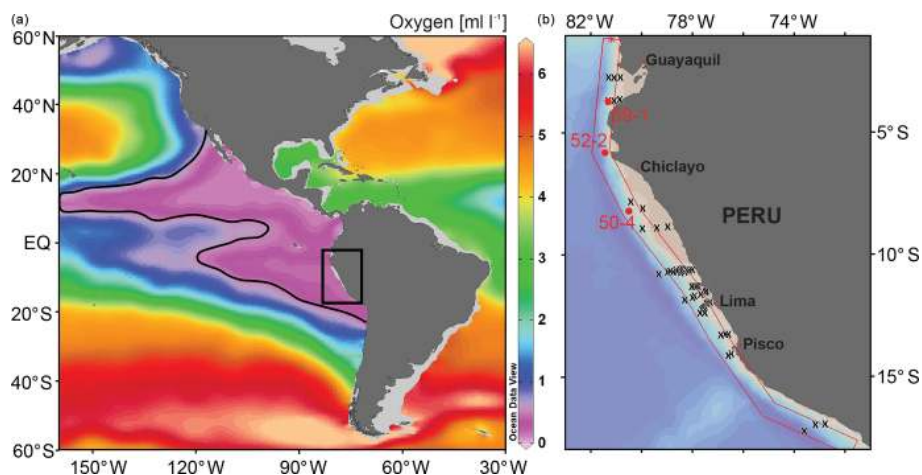
**Figure 1.** Location map of the study area (square in **a**) in the eastern equatorial Pacific and structure of the OMZ at 400 m water depths. The purple area and contour line indicate dissolved oxygen values $<0.5\,\mathrm{mL\,L^{-1}}$ (ca. $<20\,\mathrm{\mu mol\,kg^{-1}}$); World Ocean Database 2013 (Boyer et al., 2013). **(b)** Detail map of the study area showing the locations of the surface samples (x) and the sediment cores (red circles). See Fig. 2 for the sample locations in relation to water depth and the OMZ intensity.

40 °C. They were later split with an Otto microsplitter when needed, in order to attain similar total numbers of specimens, around 300 per sample (Murray, 2006). The foraminifera were dry picked, collected in Plummer cell slides, sorted by species, fixed with glue and counted. Benthic foraminiferal assemblage compositions and taxonomic references were previously reported elsewhere (Erdem and Schönfeld, 2017). Bulk sedimentary TOC (%) and $\delta^{15}$N data of core M77/2-59-1 were taken from Mollier-Vogel et al. (2019), whereas TOC and $\delta^{15}$N of core M77/2-52-2 were taken from Doering et al. (2016) and Glock et al. (2018), respectively (Table 3).

## 2.2 Surface samples and living benthic foraminifera

Information on the living (rose-bengal-stained) benthic foraminifera was compiled from four independent datasets. These studies did not report the dead (not stained) benthic foraminiferal assemblages. This is mainly due to the fact that empty (dead) foraminiferal tests are very rare and outnumbered by living specimens in surface samples from the upper Peruvian OMZ. Since the majority of the specimens in surface sediments were stained, it is not likely that there would be a substantial difference in the statistical analysis if the dead assemblage were used. The compiled dataset comprises 53 samples from the Peruvian continental shelf and slope from water depths of 48 to 2092 m between 1°45′ and 17°28′ S (Fig. 2, Table 4). Four of the samples from a transect around 12°30′ S were collected in December–January 1998 during the Panorama Expedition, leg 3a, with R/V *Melville*. Eight surface sediment samples and environmental parameters were collected from the continental shelf and uppermost slope around 12 and 14° S during different monitoring cruises with R/V *SNP 2* and *José Olaya Balandra* in August and April 2009, 2010 and 2011. For the present study, aver-

aged bottom-water oxygen values are used for these stations (for details see Cardich et al., 2015). The largest dataset was gathered from 33 surface samples collected in October to December in 2008 during R/V *Meteor* expedition M77 legs 1 and 2 (Mallon, 2012; Mallon et al., 2012). The eight most recent samples and additional data were collected in May 2017 during R/V *Meteor* expedition M137 (Sommer, 2017). The surface sediment samples in all studies comprise the topmost 10 or 30 mm. The faunal census is based on the $>63\,\mathrm{\mu m}$ size fraction. In the case of fractionated subsamples, we combined the values of different grain size fractions considering the volumes and splits reported for each subsample.

### 2.2.1 Data reduction: consideration of taphonomy

The inventory of living benthic foraminiferal species was compared with that from the sediment cores after compilation of the joint dataset. As expected, only single specimens of three agglutinated species were found in some samples from cores 50-4 and 52-2. Agglutinated species have a lower preservation potential after burial in the sediment because their organic cement is decomposed during early diagenesis or changing redox conditions (Schröder, 1988; Mackensen et al., 1990). Consequently, only species with calcareous tests were considered for further analyses. Even though agglutinated species were not used for our downcore application, they are well known for their low tolerance to oxygen minimum conditions (Bernhard and Bowser, 1999; Gooday and Rathburn, 1999; Gooday et al., 2000; Levin et al., 2002; Mallon, 2012). We therefore considered their abundances separately, and the proportions of agglutinated species in living faunas were used for a comparison of the results.

**Table 3.** Metadata of sediment cores used in this study.

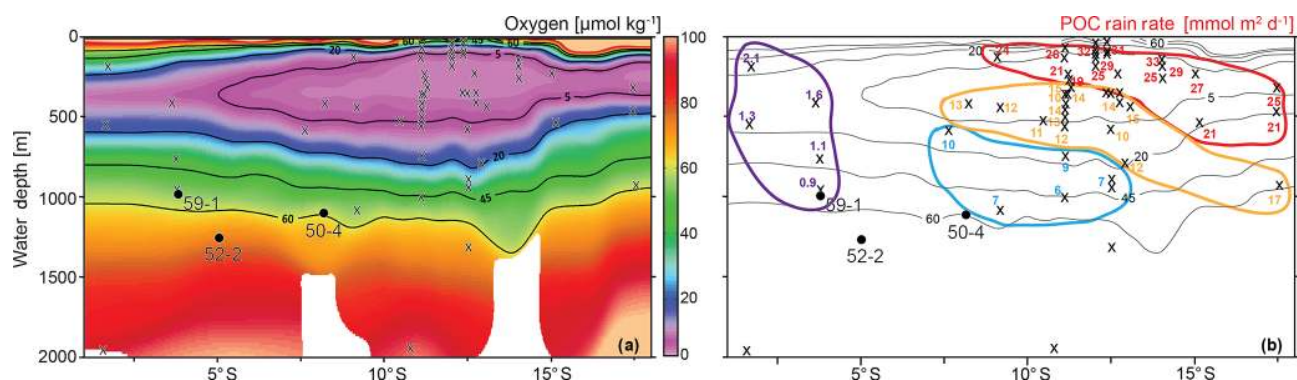| Cruise | Core name | Year | Lat (S) | Long (W) | Water depth (m) | Age model | TOC (wt %) | $\delta^{15}N_{sed}$ (‰) |
|--------|-----------|------|---------|----------|-----------------|-----------|------------|---------------------------|
| M77/2 | 059-1 | 2008 | 03°57.01′ | 81°19.23′ | 997 | Mollier-Vogel et al. (2013) | Mollier-Vogel et al. (2019) | Mollier-Vogel et al. (2019) |
| M77/2 | 052-2 | 2008 | 05°29.01′ | 81°27.00′ | 1249 | Erdem et al. (2016) | Doering et al. (2016) | Glock et al. (2018) |
| M77/2 | 050-4 | 2008 | 08°01.01′ | 80°30.10′ | 1013 | Erdem et al. (2016) | NA | NA |

NA: not available.



**Figure 2. (a)** Depth vs. latitude profile of the dissolved oxygen concentrations measured during the M77 legs 1 & 2 expeditions (red line in Fig. 1, **b** show the position of this profile; CTD data compilation after Schönfeld et al., 2015), together with the location of the surface samples (x) and the sediment cores (circles and core names). **(b)** Particulate organic carbon rain rates (RRPOC) taken from Dale et al. (2015), otherwise calculated following Martin et al. (1987). Rain rates are grouped indicating different values (<5, 5–10, 10–20 and >20 mmol m$^{-2}$ d); see text for details. Contour lines are the same as in **(a)**.

Another exception was made for *Hoeglundina elegans*. The aragonitic test of this species has a low preservation potential (Gonzales et al., 2017). *Hoeglundina elegans* was observed in four surface samples with more than 5 % abundance, but it was almost absent from the foraminiferal assemblages of sediment cores. Therefore, we excluded *H. elegans* from the census data as well. The faunal data from surface sediment and core samples were reduced accordingly.

Considering the water depths at which the sediment cores were taken (>900 m) and the depth range of our surface samples (Fig. 2), we further reduced the dataset by taking only surface samples collected from water depths >300 m into account. Species showing at least three occurrences with percentages of more than 5 % from these samples were listed and considered for further analyses. The final reduced dataset included in total 16 species from 35 samples.

### 2.2.2 Environmental data

Bottom-water oxygen concentrations ([O$_2$]$_{BW}$) were measured at the time of sampling and reported to vary between 0.0 and 100.4 µmol kg$^{-1}$ (Table 4). Dissolved oxygen concentrations at the R/V *Melville* stations around 12°30′ S were previously reported (Levin et al., 2002). For the eight R/V *SNP 2* and *José Olaya Balandra* stations, [O$_2$]$_{BW}$ data were measured on each cruise (Cardich et al., 2015). We thus considered averaged oxygen concentrations for the
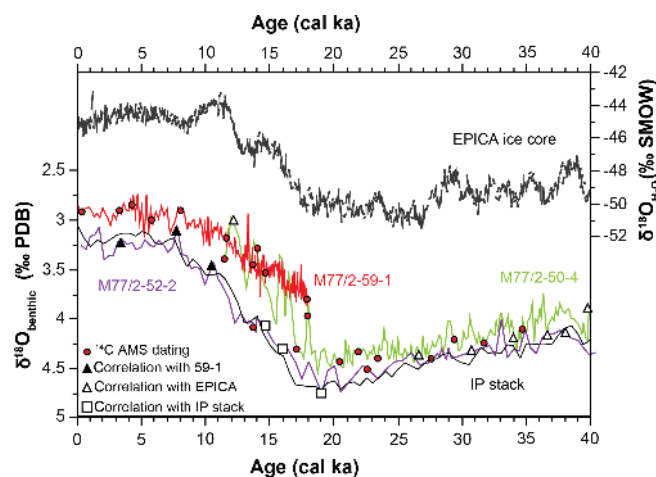


**Figure 3.** Benthic $\delta^{18}O$ isotope curves of sediment cores with age control points. Black lines are reference records: EPICA ice core (Members, 2006) and intermediate water Pacific stack (IP stack; Stern and Lisiecki, 2014). Symbols indicate the tie points used for age models. Each core is shown with different colours throughout this article.

R/V *SNP 2* and *José Olaya Balandra* stations. The [O$_2$]$_{BW}$ of the R/V *Meteor* M77 stations was taken from Mallon et al. (2012) and from a synoptic compilation of all conductivity–temperature–depth (CTD) hydrocasts from this

**Table 4.** Metadata of surface samples from the living benthic foraminifera dataset. Particulate organic carbon rain rates (RRPOC) of stations indicated in bold were taken from Dale et al. (2015); others were calculated (see text for details). Bottom-water oxygen concentrations were taken from reference publications.

| Sample | Lat, long | Water depth (m) | $[O_2]_{BW}$ ($\mu$mol kg$^{-1}$) | RRPOC (mmol m$^{-2}$ d) | Reference |
|---|---|---|---|---|---|
| Site 305 | 12°22.70′, 77°29.10′ | 305 | 0.89 | 14 | Levin et al. (2002) |
| Site 562 | 12°32.5′, 77°29.6′ | 562 | 11.61 | 10 | Levin et al. (2002) |
| Site 830 | 12°32.8′, 77°34.8′ | 830 | 37.5 | 7 | Levin et al. (2002) |
| Site 1210 | 12°40.3′, 77°38.5′ | 1210 | 79.46 | | Levin et al. (2002) |
| 540 | 11°00.01′, 77°47.41′ | 79 | 5.28 | **15.3** | Mallon (2012) |
| 694 | 9°02.97′, 79°26.88′ | 115 | 1.96 | 24.2 | Mallon (2012) |
| 470 | 11°00.00′, 77°56.61′ | 145 | 3.33 | 25.7 | Mallon (2012) |
| 772 | 1°57.01′, 81°07.23′ | 207 | 30.8 | 2.1 | Mallon (2012) |
| 676 | 11°05.01′, 78°00.91′ | 211 | 2.03 | 21 | Mallon (2012) |
| 635 | 15°04.75′, 75°44.00′ | 214 | 2.37 | 27.6 | Mallon (2012) |
| 583 | 11°06.86′, 78°03.11′ | 248 | 2.11 | 19.2 | Mallon (2012) |
| 582 | 11°09.70′, 78°04.93′ | 291 | 2.28 | 17.6 | Mallon (2012) |
| 403 | 17°26.00′, 71°51.41′ | 298 | 2.5 | 24.8 | Mallon (2012) |
| 616 | 12°22.69′, 77°29.06′ | 302 | 2.2 | **8** | Mallon (2012) |
| 473 | 11°00.03′, 78°09.95′ | 316 | 2.25 | **9.8** | Mallon (2012) |
| 449 | 11°00.00′, 78°09.97′ | 319 | 2.25 | 13.5 | Mallon (2012) |
| 744 | 3°45.01′, 81°07.29′ | 350 | 6.8 | 1.6 | Mallon (2012) |
| 716 | 7°59.99′, 80°20.51′ | 359 | 2.48 | 13.1 | Mallon (2012) |
| 482 | 11°00.02′, 78°14.17′ | 375 | 2.26 | **14** | Mallon (2012) |
| 692 | 9°17.70′, 79°37.11′ | 437 | 2.86 | 11.8 | Mallon (2012) |
| 456 | 11°00.01′, 78°19.23′ | 465 | 3.79 | 13.7 | Mallon (2012) |
| 406 | 17°28.01′, 71°52.40′ | 492 | 25.3 | 21.1 | Mallon (2012) |
| 516 | 10°59.00′, 78°21.00′ | 511 | 4.83 | 13 | Mallon (2012) |
| 553 | 10°26.38′, 78°54.7′ | 521 | 4.83 | 10.7 | Mallon (2012) |
| 421 | 15°11.39′, 75°34.81′ | 522 | 13.83 | 20.8 | Mallon (2012) |
| 767 | 1°53.49′, 81°11.75′ | 526 | 19 | 1.3 | Mallon (2012) |
| 487 | 11°00.00′, 78°23.17′ | 579 | 8.59 | 12.2 | Mallon (2012) |
| 723 | 7°52.01′, 80°31.36′ | 627 | 8.23 | 9.7 | Mallon (2012) |
| 459 | 11°00.02′, 78°25.6′ | 697 | 15.72 | **9** | Mallon (2012) |
| 757 | 3°51.01′, 81°15.49′ | 700 | 40 | 1.1 | Mallon (2012) |
| 622 | 12°32.74′, 77°34.73′ | 823 | 27.67 | 7 | Mallon (2012) |
| 410 | 17°38.40′, 71°58.23′ | 918 | 58 | 17 | Mallon (2012) |
| 753 | 3°56.95′, 81°19.16′ | 995 | 54 | 0.9 | Mallon (2012) |
| 549 | 10°59.81′, 78°31.26′ | 1004 | 44.78 | **5.9** | Mallon (2012) |
| 684 | 9°17.69′, 79°53.86′ | 1105 | 56.63 | 7.1 | Mallon (2012) |
| 669 | 10°53.22′, 78°46.38′ | 1923 | 98.35 | | Mallon (2012) |
| 776 | 1°45.14′, 82°37.47′ | 2092 | 100.39 | | Mallon (2012) |
| C1 | 12°01.90′, 77°13.07′ | 48 | 10.01 | | Cardich et al. (2015) |
| C2 | 12°02.76′, 77°17.27′ | 94 | 5.85 | | Cardich et al. (2015) |
| C3 | 12°02.34′, 77°22.53′ | 117 | 4.8 | 32.4 | Cardich et al. (2015) |
| P1 | 14°01,20′, 76°18,78′ | 120 | 1.80 | 33.2 | Cardich et al. (2015) |
| C4 | 12°02.93′, 77°29.01′ | 143 | 6.08 | 29.1 | Cardich et al. (2015) |
| C5 | 12°02.22′, 77°39.07′ | 175 | 6.08 | 26.1 | Cardich et al. (2015) |
| P2 | 14°04.32′, 76°25.20′ | 180 | 1.58 | 29.2 | Cardich et al. (2015) |
| P3 | 14°07.50′, 76°30.54′ | 300 | 2.70 | 24.8 | Cardich et al. (2015) |
| M137-681 | 12°13.51′, 77°10.77′ | 74 | 5.69 | | This study |
| M137-641 | 12°16.67′, 77°14.99′ | 128 | 1.6 | 30 | This study |
| M137-695 | 12°16.78′, 77°14.98′ | 130 | 1.11 | 30 | This study |
| M137-608 | 12°23.26′, 77°24.28′ | 244 | 0.00 | 21 | This study |
| M137-776 | 12°24.89′, 77°26.29′ | 303 | 0.02 | 19.3 | This study |
| M137-788 | 12°27.19′, 77°29.29′ | 413 | 0.00 | 16.4 | This study |
| M137-735 | 12°38.14′, 77°20.74′ | 489 | 2.05 | 14.9 | This study |
| M137-670 | 12°31.36′, 77°34.99′ | 752 | 16.75 | 11.8 | This study |

area (Schönfeld et al., 2015). The $[O_2]_{BW}$ of the R/V *Meteor* M137 stations was extracted from the expedition dataset (Gerd Krahmann, personal communication, 2018). Bottom-water oxygen concentrations around the lower boundary in the region are relatively stable throughout the year, whereas the upper boundary is quite dynamic (Paulmier and Rioz-Pino, 2009). We compared the $[O_2]_{BW}$ from stations close to each other, and those sampling campaigns took place in different years and seasons. The only difference was observed at two 820 m stations (January 1998 vs. May 2017; ca. 10 μmol kg$^{-1}$); the other stations did not show significant contrast between different sampling periods (Table 4). Therefore, we consider the reduced living assemblage data to be least affected by seasonality of $[O_2]_{BW}$.

Rain rates of particulate organic carbon (RRPOC; mmol m$^{-2}$ d) for six of the stations were taken directly from Dale et al. (2015; Table 4). The rain rates for the other stations were estimated by using equations provided for water depths between 100 and 1000 m (Martin et al., 1987; Dale et al., 2015). Different primary productivity values were used for the RRPOC calculations. For the region around 11–12° S, values reported in the Supplement of Dale et al. (2015) were used since the measurements were done close to sampling during the M77 expedition (Mallon et al., 2012). For the region around and south of 15° S, values reported by Martin et al. (1987) were considered. For the northern part of the study area, estimates from Pennington et al. (2006) were used.

## 2.3 Statistical analyses

We standardized the reduced data matrix by calculating the proportions of the involved species referring to the total calcareous (calcitic) species of each sample as described above. Relative abundances (percentages) were preferred instead of absolute abundances (individuals per cubic centimetre) since this information would create an inconsistency when applied to surface sediment samples and to fossil sediments in the same manner. Diversity and dominance values were calculated for the reduced calcareous (calcitic) assemblages applying centred bootstrapping, together with $Q$-mode hierarchical cluster analysis and canonical correspondence analysis (CCA), including comparison with the environmental variables $[O_2]_{BW}$ and RRPOC.

All statistical and diversity analyses were performed with the PAleontological STatistics (PAST) software, version 3.11 (Hammer et al., 2001). $Q$-mode hierarchical cluster analysis was applied using the unweighted pair group method (UP-GMA) based on a Bray–Curtis similarity matrix. Canonical correspondence analysis (CCA) was performed on the same datasets to see the relation between the species, stations and environmental variables (Fig. S3 in the Supplement). Additionally, multiple regression analysis was applied, and the significance was assessed in order to evaluate the reliability for downcore applications. Coefficients and intercept value from the multiple regression analysis were later used as data

entry for a polynomial transfer function (Supplement) to calculate past bottom-water oxygen concentrations ($[O_2]_{BW}$) from foraminiferal assemblages of sediment core samples.

## 3 Results

### 3.1 Living benthic foraminiferal distributions

The entire dataset of living calcareous benthic foraminifera from the Peruvian margin comprised 53 surface sediment samples and 127 different calcareous (calcitic) species. When the oxic (>45 μmol kg$^{-1}$), dysoxic (5–45 μmol kg$^{-1}$) and microxic (<5 μmol kg$^{-1}$) classification (Table 1) was applied to this dataset, 27 samples were classified as microxic, 20 samples were classified as dysoxic and the remaining 6 samples were classified as oxic (Fig. 4). The diversity of calcareous species and the relative abundance of the total of agglutinated species increased with bottom-water oxygen. In particular, a marked increase in the proportion of agglutinated species was observed at stations with $[O_2]_{BW}$ >15 μmol kg$^{-1}$, and a further increase was recorded around 40 μmol kg$^{-1}$. The proportion of the agglutinated taxa was more than 50 % at sampling stations under oxic conditions. The assemblages were, however, less diverse compared to dysoxic samples, as depicted by low Fisher alpha indices and the dominance of single species. This pattern implies that these six oxic stations did not represent the total calcareous taxa very well; neither do the stations in the reduced dataset of 16 species and 35 samples that we statistically analysed. The microxic samples showed less diverse assemblages with higher dominance, whereas the dysoxic samples showed higher diversities and a lower dominance. The Fisher alpha diversity indices were lower and dominance was higher at stations under dysoxic conditions where the living faunas were dominated by Bolivinids (Fig. 4).

In the centre of the OMZ, at microxic stations, the most abundant species was *Bolivina seminuda* (Fig. S1), followed by *B. costata*, *B. interjuncta*, *B. spissa* and *Bolivinita minuta* with increasing oxygen concentrations. *Uvigerina peregrina* became the most abundant species outside the OMZ core, showing similar trends as agglutinated species and other calcareous species which increased markedly as well. *Pyrgo murrhyna* and *Melonis barleeanum* were observed only at oxic stations. $Q$-mode hierarchical cluster analysis on the entire census data (53 samples and 127 calcareous species) indicated three clusters (Fig. S2). The census dataset was later reduced to the most abundant 16 species from stations deeper than 300 m. All of the species from this subset were grouped in two clusters (Fig. S2a, b). Application of CCA to these abundant species showed similar results (Figs. S3 and S4). Most of the samples and species grouped together as indicated by their positive loading of axis 2. Overall, lower $[O_2]_{BW}$ and higher RRPOC did not show an eye-catching relation as expected. When multiple regression
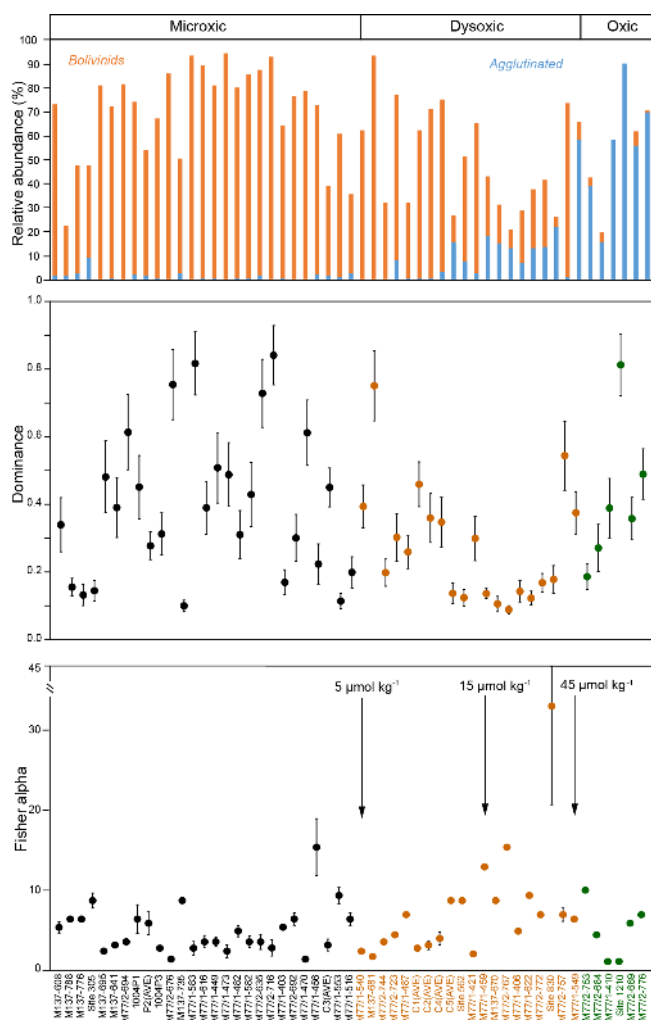
**Figure 4.** Relative abundances of Bolivinids and agglutinated species at each station in relation with the bottom-water oxygen measured during sampling. Oxic ($>45\,\mu\mathrm{mol\,kg}^{-1}$), dysoxic ($5$–$45\,\mu\mathrm{mol\,kg}^{-1}$) and microxic ($<5\,\mu\mathrm{mol\,kg}^{-1}$) classification was applied to these samples, and the colours green, orange and black were used respectively as indicators of the thresholds (see also Table 1). Dominance and Fisher alpha diversity indices were also calculated for the same samples.

results were used to compare these observations, the fitted $[\mathrm{O_2}]_{\mathrm{BW}}$ showed a significant correlation with measured values at the sampling stations whereas the RRPOC estimates did not: $R^2 = 0.82$, $p < 0.05$ and $R^2 = 0.53$, $p = 0.31$, respectively (Fig. 5 and Table 5).

### 3.2 Application of $[\mathrm{O_2}]_{\mathrm{BW}}$ estimates to sediment cores

Erosion, reworking and high energetic bottom conditions prevail at the continental slope of the Peruvian margin. The Holocene from core 50-4 was missing (Erdem et al., 2016), and due to the high sedimentation rates, core 59-1 covers only the late Holocene (LH), early Holocene (EH), Bølling

Allerød/Antarctic Cold Reversal (BA/ACR), and Heinrich Stadial-1 (HS1). Consequently, it was only possible to compare these time intervals in all of the sediment cores. In the following, we describe the results of $[\mathrm{O_2}]_{\mathrm{BW}}$ quantification for each core separately, from south to north. We abstained from applying the same approach to reconstruct past RRPOC for the downcore records because the regression analyses did not show a significant correlation. Additionally, these cores were recovered around or deeper than 1000 m, which was the maximum depth for any reliable RRPOC calculations.

Core M77/2-50-4 was collected from 1013 m water depth, and the $[\mathrm{O_2}]_{\mathrm{BW}}$ was 52 $\mu\mathrm{mol\,kg}^{-1}$ during the time of sampling. In total, 20 samples were analysed covering the time intervals BA/ACR, HS1 and LGM; the Holocene was missing in this core. Among the 138 benthic foraminiferal species identified, only one was agglutinated (*Dorothia goesi*) and occurred as a single specimen in samples from the early HS1 and LGM. The estimated paleo-oxygen concentrations ranged from 35 to 43 $\mu\mathrm{mol\,kg}^{-1}$ during the LGM, varied between 21 and 40 $\mu\mathrm{mol\,kg}^{-1}$ during the HS1, and varied between 9 and 15 $\mu\mathrm{mol\,kg}^{-1}$ during the BA/ACR. Deviations ranged from 9 to 17 $\mu\mathrm{mol\,kg}^{-1}$. Core M77/2-52-2 was collected from 1249 m water depth. The $[\mathrm{O_2}]_{\mathrm{BW}}$ was 74 $\mu\mathrm{mol\,kg}^{-1}$ at the core location during sampling. In total, 27 samples were analysed, and 170 species were identified of which three were agglutinated. The estimated $[\mathrm{O_2}]_{\mathrm{BW}}$ indicated stable conditions during the LGM with values ranging from 52 to 61 $\mu\mathrm{mol\,kg}^{-1}$, which was followed by a decrease from 56 to 46 $\mu\mathrm{mol\,kg}^{-1}$ from mid-HS1 to mid-BA/ACR and a much more distinct decrease at the end of BA/ACR from 53 to 10 $\mu\mathrm{mol\,kg}^{-1}$. After the deglaciation, the fluctuations were weaker, indicating rather stable conditions with values of 13 to 30 $\mu\mathrm{mol\,kg}^{-1}$ during the EH and 23 to 32 $\mu\mathrm{mol\,kg}^{-1}$ during the LH. The standard deviations (1SD) ranged from 8 to 20 $\mu\mathrm{mol\,kg}^{-1}$. Core M77/2-59-1 was recovered from the northernmost part of the study area, from 997 m water depths, and the $[\mathrm{O_2}]_{\mathrm{BW}}$ was 54 $\mu\mathrm{mol\,kg}^{-1}$ during sampling. The core location has been under the influence of strong riverine input. The sedimentation rates throughout the core were 50 and 170 cm ka$^{-1}$, rather high compared to the other cores (Mollier-Vogel et al., 2013). Because of these high sedimentation rates, the LGM was not retrieved by this core. In total, 20 samples were analysed and 161 species were identified. Agglutinated species were scarce but present. They were more frequent in samples older than 9 cal ka. The estimated $[\mathrm{O_2}]_{\mathrm{BW}}$ ranged from 34 to 60 $\mu\mathrm{mol\,kg}^{-1}$ during HS1, from 63 to 18 $\mu\mathrm{mol\,kg}^{-1}$ during the BA/ACR, and varied between 11 and 30 $\mu\mathrm{mol\,kg}^{-1}$ during the EH and between 3 and 25 $\mu\mathrm{mol\,kg}^{-1}$ during the LH. One sample showed a negative value, obviously an artefact of the method. Overall standard deviations were calculated as ranging from 9 to 28 $\mu\mathrm{mol\,kg}^{-1}$. When the average values were considered in each time interval, the decrease from HS1 to the end of BA/ACR was 16 $\mu\mathrm{mol\,kg}^{-1}$ in core 50-4, 20 $\mu\mathrm{mol\,kg}^{-1}$ at core 52-2 and only 6 $\mu\mathrm{mol\,kg}^{-1}$ in core 59-1. The difference

**Table 5.** List of the living benthic foraminifera species which were considered in the transfer function, regression coefficients and $1\sigma$ errors that were calculated with multiple regression analyses.

| | $[O_2]_{BW}$ ($\mu$mol kg$^{-1}$) | | RRPOC (mmol m$^{-2}$ d) | |
|---|---|---|---|---|
| | Coeff. | $1\sigma$ | Coeff. | $1\sigma$ |
| Constant | 73.83 | 7.249 | 9.6117 | 2.6353 |
| *Bolivina costata* | −1.011 | 0.34144 | 0.26655 | 0.12413 |
| *Bolivina interjuncta* | −1.0887 | 0.26074 | 0.092808 | 0.094787 |
| *Bolivina plicata* | −1.4618 | 0.89245 | −0.12367 | 0.32443 |
| *Bolivina seminuda* | −0.70357 | 0.1895 | 0.018734 | 0.068888 |
| *Bolivina spissa* | −0.43921 | 0.24046 | −0.1654 | 0.087413 |
| *Bolivinita minuta* | −2.4131 | 0.91546 | −0.10672 | 0.3328 |
| *Cancris carmenensis* | −0.85979 | 0.4664 | 0.099572 | 0.16955 |
| *Cassidulina crassa* | −1.8999 | 1.1847 | 0.17166 | 0.43069 |
| *Cassidulina delicata* | −0.80009 | 0.45983 | −0.13439 | 0.16716 |
| *Epistominella obesa* | −0.4445 | 0.95982 | 0.074865 | 0.34893 |
| *Epistominella pacifica* | −0.1219 | 0.34751 | −0.02116 | 0.12633 |
| *Fursenkoina fusiformis* | −1.0253 | 1.7209 | −0.74266 | 0.6256 |
| *Gyroidina soldanii* | −1.7552 | 0.54323 | −0.27674 | 0.19748 |
| *Suggrunda porosa* | −1.7787 | 1.1695 | 0.34883 | 0.42516 |
| *Uvigerina peregrina* | −0.00054 | 0.561 | 0.2497 | 0.20394 |
| *Valvulineria glabra* | 0.2821 | 1.4686 | 0.29553 | 0.5339 |

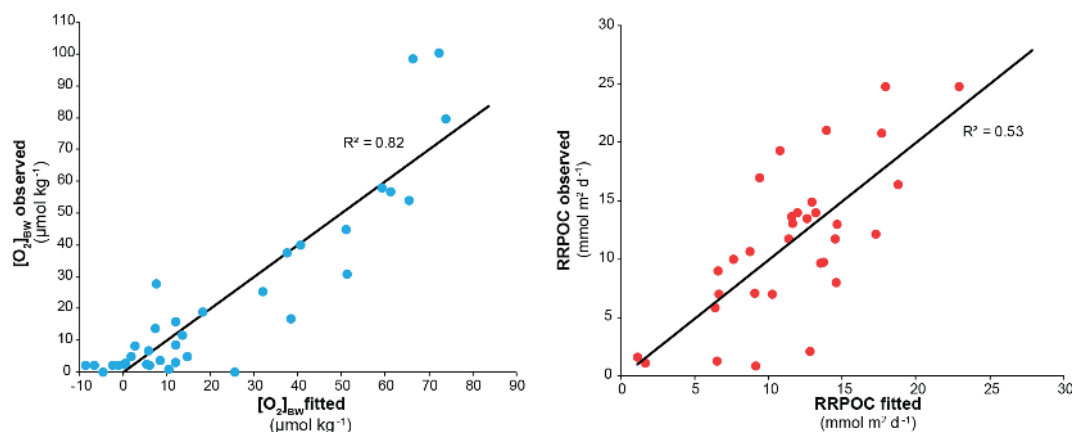| | $R^2$ | $p$ | |
|---|---|---|---|
| $[O_2]_{BW}$ ($\mu$mol kg$^{-1}$) | 0.824 | 0.00056 | |
| RRPOC (mmol m$^{-2}$ d) | 0.5293 | 0.3131 | |



**Figure 5.** Graphs showing the regression results applied to the living benthic foraminifera dataset for bottom-water oxygen ($[O_2]_{BW}$) and POC rain rates (RRPOC).

between the BA/ACR and the early Holocene $[O_2]_{BW}$ was around 11 $\mu$mol kg$^{-1}$ at core 52-2 and around 24 $\mu$mol kg$^{-1}$ at core 59-1.

## 4 Discussion

### 4.1 Living benthic foraminifera in relation to OMZ settings

Similar to previous observations from other modern OMZs, benthic foraminifera living in the Peruvian OMZ showed high population densities and low diversity in the centre. Certain species, predominantly Bolivinids, were observed to be

the most abundant species here. They are known for their high tolerance to suboxic and even anoxic conditions (Table 2; Mullins et al., 1985; Schumacher et al., 2007; Piña-Ochoa et al., 2010; Glock et al., 2011; Mallon et al., 2012; Cardich et al., 2015). In the vicinity of the OMZ core, around the boundary, a more diverse assemblage (cluster A; Fig. S2) was observed. Considering the environmental information gathered on some of the species of this group, such as *Bolivina spissa*, *Bolivinita minuta*, *Cassidulina delicata*, *Epistominella pacifica* and *Uvigerina peregrina* (Table 2), the assemblage seemingly represented a transitional community which reacted to a broader range of environmental variables including increasing water depths, oxygen content and organic carbon content. The living taxa from stations below the lower boundary of the OMZ indicated a much more diverse assemblage (cluster B; Fig. S2). This assemblage involved mostly Miliolids which are known for their intolerance to low oxygen (e.g. Caulle et al., 2014). Agglutinated species dominated the whole assemblage from these samples, which again mirrors rather oxic conditions. The data are in good agreement with previous observations on the low tolerance of agglutinated species to oxygen-depleted conditions ($<0.2 \, \text{mL} \, \text{L}^{-1} = \sim 9 \, \mu\text{mol} \, \text{kg}^{-1}$; Gooday et al., 2000). In the CCA on the living fauna, this Miliolid-associated assemblage (cluster B), together with the agglutinated species, showed a positive relation with $[O_2]_{BW}$ (Fig. S3). Similar trends of such different assemblages in relation with changing oxygen and organic matter were also observed in the Arabian Sea (Jannink et al., 1998; Caulle et al., 2014). Even though there are different species involved in the assemblages representing the OMZ core (microxic), around the boundary of the OMZ (dysoxic) and outside the OMZ (oxic), the transitional appearance of these assemblages from low diversity to high density to more diverse and cosmopolitan assemblages indicates strong similarities.

Comparison of living taxa in different OMZ settings revealed that each OMZ has its own genuine assemblages. The most abundant species were not observed at similar abundances in other OMZs, indicating that they are specifically adapted to the conditions in these regions. For example, *Bolivina dilatata* is dominant in the Arabian OMZ (Jannink et al., 1998), and *Bolivina costata* is frequent in the core of the Peruvian OMZ (this study; Cardich et al., 2012; Mallon et al., 2012). While *Bolivina dilatata* is widely distributed in the Atlantic Ocean too, including the Mediterranean, *Bolivina costata* is seemingly endemic to the western South American margin. This "trapped" occurrence might be due to the structure and shape of the OMZ, prevailing for more than 0.5 million of years, and the strong adaptation of these assemblages to conditions during a long time (e.g. Heinze and Wefer, 1992). Similar assumptions were made for the OMZ core assemblages in the northern Arabian Sea (Jannink et al., 1998). Therefore, expecting to find the same specific species within the same oxygen range in different OMZs is potentially misleading. Although there

are not many frequent species observed in different OMZs, *Bolivina seminuda* and *Bulimina exilis* are within the few common species (Table 2; Bernhard et al., 1997; den Dulk et al., 1998; Cardich et al., 2015). Elevated proportions of these two species could be used as an extremely low-bottom-water-oxygen indicator in downcore records (e.g. McKay et al., 2015; Praetorius et al., 2015; Tetard et al., 2017). Additionally, total numbers of the Miliolids could be oxic condition indicators as previously suggested (den Dulk et al., 2000), but this approach would not produce sensible results outside OMZ settings. Accordingly, comparisons of relative abundances of these low-oxygen-tolerant and low-oxygen-intolerant species in the fossil record might be used in determining dysoxic–oxic transitions (e.g. Kaiho, 1994; Cannariato et al., 1999; Schmiedl et al., 2003; Tetard et al., 2017; Balestra et al., 2018).

## 4.2 Peruvian margin oxygen history since the LGM

The records revealed a distinct overall decrease in $[O_2]_{BW}$ during deglaciation around the lower OMZ boundary. The spatial delineation of oxygenation changes between the LGM and the Holocene is limited since our records do not fully cover all the considered time intervals. When the records were stacked, the estimates showed a decreasing trend starting from the LGM, a distinct drop during the deglaciation with fluctuations from the HS1 to the BA/ACR and a slight increase followed by relatively stable concentrations during the Holocene. Nonetheless, Holocene $[O_2]_{BW}$ values were still lower than those of the LGM. This trend is consistent with other results reported in reviews of bottom-water deoxygenation during the deglaciation in the eastern Pacific Ocean (Jaccard and Galbraith, 2012; Moffitt et al., 2015). Both reviews consider different proxies (e.g. lamination, $\delta^{15}$N, redox-sensitive elements) which are known to indicate oxygen-depleted conditions as recorded by sediment cores from above 500 m depth off Peru. When the records are evaluated individually, relatively stable LGM $[O_2]_{BW}$ values at both available records were followed by a continuous decrease during the deglaciation in the southernmost core. The $[O_2]_{BW}$ from the northern cores suggested that bottom waters experienced increased oxygen levels during the early BA/ACR. This is potentially due to weakening of surface productivity or, considering the positions of both cores on the continental slope (900–1300 m), due to intermediate water mass advection of oxygen-rich waters. Water mass contributions might have changed during the deglaciation at these cores sites as previously reported (e.g. Antarctic Intermediate Water (AAIW) from the south and North Pacific Intermediate Water (NPIW) from the north; Bova et al., 2018). Overall, the highest decrease was observed in the deepest core, implying that the absolute changes at the lower boundary were larger than in the shallower depths. Another quantification approach compared Fe concentrations and Mo/U ratios in core M77/2-24-5 from the upper slope off Peru at 11° S and
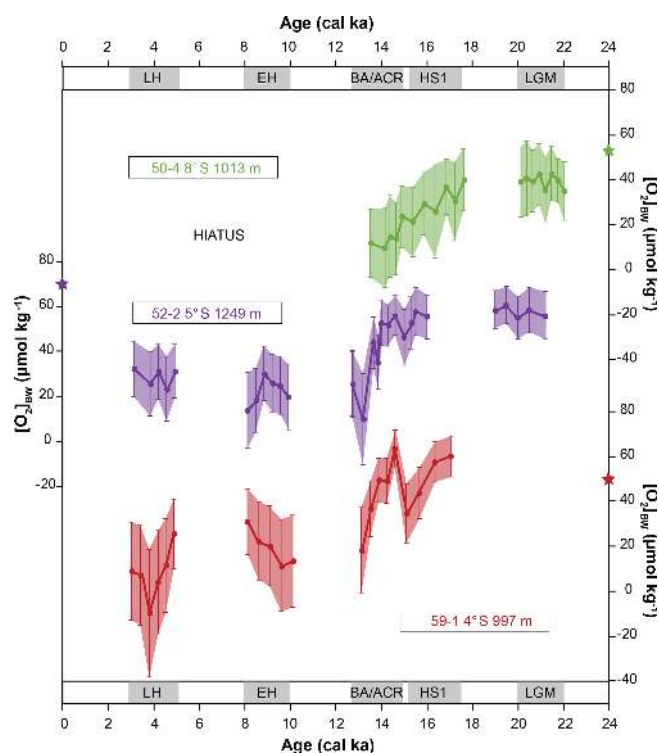
**Figure 6.** Comparison of the estimated bottom-water oxygen concentrations $[O_2]_{BW}$ applied to three sediment cores from south to north. Stars indicate the modern $[O_2]_{BW}$ measured during sampling in 2008. Error bars are calculated using $1\sigma$ errors using values shown in Table 5 and using equations described in the Supplement.

210 m water depths (Scholz et al., 2014). They found a drop of 5 to 10 $\mu$mol L$^{-1}$ during the deglaciation, suggesting that when the OMZ intensifies (or diminishes) the change is profound around its borders and the conditions are rather stable close to its centre. More recently, a modelling approach quantified oxygen concentrations during the deglaciation and reported similar estimates with relatively stable conditions in shallower depths and a larger decrease in intermediate and deep waters (their Fig. 6; Yamamoto et al., 2019).

The downcore distribution of benthic foraminiferal species that were not included in the quantification approach provided further corroborating evidence. For instance, the disappearance of *Prygo murrhyna* and agglutinated species after HS1 at core 50-4 and the increasing abundances of *B. costata* during the same time interval suggested that bottom-water conditions successively became dysoxic (Erdem and Schönfeld, 2017). Similarly, the presence of *P. murrhyna* and agglutinated species throughout core 52-2 suggested that the prevailing oxygen levels have been moderate during the considered time intervals. Due to hiatus and sampling resolution, our assessments for the Holocene are limited. In addition, large standard deviations observed in the northernmost core 59-1 raised questions about the applicability of the method for the Holocene at this core (Fig. 6). Nevertheless, both

Holocene records of cores 59-1 and 52-2 suggested a trend of increasing bottom-water oxygenation that is in accordance with recently published results from the region (Salvatteci et al., 2016, 2018; Mollier-Vogel et al., 2019). Moreover, it is possible that bottom waters became more oxic after the late Holocene as reported for the shelf during the last 100–150 years (Cardich et al., 2019). However, we cannot comment further for the rest of the Holocene $[O_2]_{BW}$ trend on the basis of currently available information.

Finally, the estimated values together with standard deviations indicated negative values, which might be considered a challenge for the applicability of this approach. Once we looked closer, only one data point at core M77/2-59-1 indicated a negative value (Table S1 in the Supplement), which is not physically possible. The negative values shown on the scale bars (in Fig. 6) are inferred by the large standard deviations from a few samples. This is potentially an artefact of the transfer function where the estimates are biased towards lower values, because the majority of reference surface samples are from depths shallower than the sediment cores investigated, hence at lower oxygen concentrations. And yet, our estimations are within a realistic range of positive $[O_2]_{BW}$ within the statistical uncertainty. Moreover, we are confident in the $[O_2]_{BW}$ differences in each time interval considered, even though the absolute estimates for each sample might be biased because of the dominance of the low-oxygen samples in the reference dataset. As with any new approach, precision will improve as additional samples and more species information become available.

### 4.3 Comparison with other proxies and records from the region

Total organic carbon content (TOC (wt %)) from cores 52-2 and 59-1 showed an increasing trend with the onset of the deglaciation followed by relatively similar trends during the Holocene (Fig. 7; Doering et al., 2016; Mollier-Vogel et al., 2019). Higher TOC values during the Holocene suggested higher preservation and thus enhanced productivity and relatively low oxygen values prevailing at core locations since the EH in comparison to the LGM. Meanwhile, sedimentary $\delta^{15}N$ values from both cores indicated a higher surface productivity and/or water column denitrification and hence a stronger OMZ during the deglaciation compared to the LGM and the Holocene (Glock et al., 2018; Mollier-Vogel et al., 2019). The opposite $\delta^{15}N_{sed}$ trend observed at both cores during the BA/ACR is intriguing. In the case of more oxygenated bottom waters, as depicted by our $[O_2]_{BW}$ estimates from cores 59-1 and 52-2, $\delta^{15}N_{sed}$ is expected to be lower as observed at core 52-2. This opposing trend suggests that different regional dynamics had an interfering impact on N dynamics at core 59-1 during the early BA/ACR. On the other hand, TOC values from both records are in agreement with bottom-water oxygenation estimates from our $[O_2]_{BW}$ approach during this period.
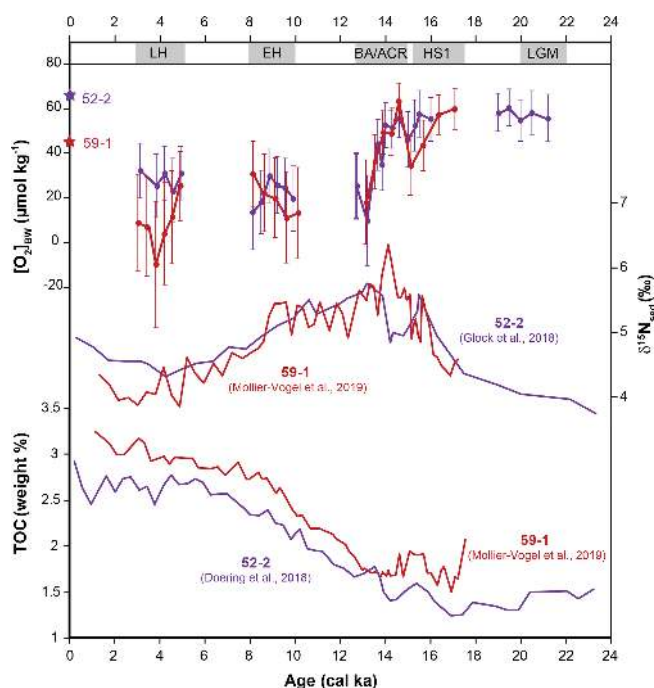
**Figure 7.** Comparison of $[O_2]_{BW}$ estimated concentrations with bulk sedimentary $\delta^{15}N$ and TOC (wt %) from the same cores (data are available for cores M77/2-59-1 and M77/2-52-2).

Later in the record both cores indicated a distinct drop in the bottom-water oxygen concentrations that were also mirrored by the increasing denitrification during the BA/ACR as displayed by high $\delta^{15}N_{sed}$ values. Other redox and productivity proxies from the region revealed similar trends. Laminated sediments indicating $[O_2]_{BW}$ of $<7\,\mu mol\,kg^{-1}$ (e.g. Schönfeld et al., 2015) were observed to be widest in extent during HS1, in particular on the continental shelf and upper slope between 10 and 18° S (Erdem et al., 2016). Stacked records from the Peruvian margin at 14° S revealed a correlation between enhanced productivity and low bottom-water oxygen as indicated by increasing Mo/U values within the laminated sediments during the HS1 period (Salvatteci et al., 2016). Enhanced surface productivity, increasing denitrification and bottom-water deoxygenation during the early deglaciation were observed in various records from the eastern equatorial Pacific (Pedersen, 1983; Pedersen et al., 1988; Hendy and Pedersen, 2006; Martinez and Robinson, 2010; Bova et al., 2018). The distinct increase in relative abundances of the phytodetritus bloom-feeding *Epistominella exigua* in cores 52-2 and 59-1 during the deglaciation supported these observations, indicating an enhanced organic matter flux to the sea floor (Erdem and Schönfeld, 2017). Nevertheless, the highest percentages of *E. exigua* at core 52-2 were recorded when the bottom-water oxygenation indicated more or less stable conditions. This decoupling of productivity and deoxygenation suggested that bottom-water deoxygenation did not always co-occur with enhanced sur-

face productivity at the core location. The discrepancy might be a corroborating evidence that parameters other than primary productivity were influencing the oxygen dynamics in the Peruvian OMZ as they do today, for instance ventilation of intermediate waters or changes in the hydrodynamics (Karstensen et al., 2008; Brandt et al., 2015). However, it should be kept in mind the Peruvian margin potentially represents a much more complex structure in terms of productivity as it is mirrored in biogenic opal and $\delta^{30}Si$ records (Doering et al., 2016) as well as the impact of different intermediate water masses and stratification (Bova et al., 2015, 2018). The same caution should be applied to our *E. exigua* records. The species was observed in the northern cores but not in core 50-4 situated much closer to the main upwelling area. This might be explained by the upper food flux tolerance limit of ca. $200\,g\,C\,m^{-2}\,yr^{-1}$ for this species (Altenbach et al., 1999: their Fig. 6). Differences observed in bottom-water oxygenation in our records might also be an indication of changing dynamics in the mixed layer (e.g. primary productivity and upwelling) instead of changes in intermediate water masses. However, further and broader investigation focusing on other records and proxies is needed to confirm this. Even though our estimated $[O_2]_{BW}$ values were lower than anticipated, the quantification approach is consistent in terms of absolute changes and coherent with other proxies. Our data and comparisons with other proxies indicated an expansion of the northern part of the Peruvian OMZ in terms of thickness and wideness during the last deglaciation with a decrease in $[O_2]_{BW}$ of $30\,\mu mol\,kg^{-1}$ at its lower boundary.

## 5 Conclusions

The use of benthic foraminiferal assemblages as a bottom-water oxygenation proxy has been under debate since the oxygen deficiency indicator species can be found in many other environments as well. When certain thresholds are applied, for instance microxic ($<5\,\mu mol\,kg^{-1}$), dysoxic ($5–45\,\mu mol\,kg^{-1}$) and oxic ($>45\,\mu mol\,kg^{-1}$), benthic foraminiferal assemblages were observed, indicating similar transitional trends in different oxygen minimum zone settings world-wide, even though they are composed of different species. The present study reports an extensive dataset based on four independent studies of living (rose-bengal-stained) benthic foraminiferal distributions from the continental shelf and slope off Peru. The faunal distribution data were compared with bottom-water oxygen concentrations ($[O_2]_{BW}$) measured during the sampling periods. Certain species and assemblages showed a much better correlation with $[O_2]_{BW}$ than with rain rates of particulate organic carbon (RRPOC). Application of a multiple regression analysis with $[O_2]_{BW}$ as the dependant variable indicated that the foraminiferal assemblages along the Peruvian margin are rather governed by oxygen availability than by the deposition of particulate organic matter. The correlation

with $[O_2]_{BW}$ was significant ($R^2 = 0.82$; $p < 0.05$); therefore we applied the transfer function to three sediment cores taken from the lower boundary of the Peruvian Oxygen Minimum Zone (OMZ) in order to quantify the past $[O_2]_{BW}$. The data revealed a drop in $[O_2]_{BW}$ of $30\,\mu\mathrm{mol\,kg^{-1}}$ at the lower boundary of the OMZ during the last deglaciation. The overall bottom-water oxygen trend revealed a distinct drop during the deglaciation, with a slight increase around 15 cal ka observed in the northern cores. The largest decrease in $[O_2]_{BW}$ was observed at the later part of the deglaciation, which was followed by a slight increase as recorded in the northern cores during the Holocene. This general trend is in line with previous paleo-oxygenation proxy records at intermediate depths from the eastern Pacific Ocean, supporting the viability of the benthic foraminiferal approach.

*Data availability.* Data presented in this study can be accessed through the following link: https://doi.org/10.1594/PANGAEA.901840 (Erdem et al., 2019).

*Supplement.* The supplement related to this article is available online at: https://doi.org/10.5194/bg-17-3165-2020-supplement.

*Author contributions.* ZE, JS and NG designed and conceptualized the project. JC, AER, MEP, JS and ZE accomplished the data collection. ZE and NG completed data analysis. ZE wrote the manuscript. All authors contributed to editing of the manuscript.

*Competing interests.* The authors declare that they have no conflict of interest.

*Special issue statement.* This article is part of the special issue "Ocean deoxygenation: drivers and consequences – past, present and future (BG/CP/OS inter-journal SI)". It is not associated with a conference.

## References

Altenbach, A. V., Pflaumann, U., Schiebel, R., Thies, A., Timm, S., and Trauth, M.: Scaling percentages and distributional patterns of benthic foraminifera with flux rates of organic carbon, J. Foramin. Res., 29, 173–185, 1999.

Alve, E. and Bernhard, J. M.: Vertical Migratory Response of Benthic Foraminifera to Controlled Oxygen Concentrations in an Experimental Mesocosm, Mar. Ecol. Prog. Ser., 116, 137–151, https://doi.org/10.3354/meps116137, 1995.

Baas, J. H., Schönfeld, J., and Zahn, R.: Mid-depth oxygen drawdown during Heinrich events: evidence from benthic foraminiferal community structure, trace-fossil tiering, and benthic $\delta^{13}$C at the Portuguese Margin, Mar. Geol., 152, 25–55, 1998.

Balestra, B., Krupinski, N. B. Q., Erohina, T., Fessenden-Rahn, J., Rahn, T., and Paytan, A.: Bottom-water oxygenation and environmental change in Santa Monica Basin, Southern California during the last 23 kyr, Palaeogeogr. Palaeocl., 490, 17–37, 2018.

Barmawidjaja, D. M., Jorissen, F. J., Puskaric, S., and Van der Zwaan, G. J.: Microhabitat selection by benthic foraminifera in the northern Adriatic Sea, J. Foramin. Res., 22, 297–317, 1992.

Bernhard, J. M. and Bowser, S. S.: Benthic foraminifera of dysoxic sediments: chloroplast sequestration and functional morphology, Earth-Sci. Rev., 46, 149–165, 1999.

Bernhard, J. M. and Sen Gupta, B. K.: Foraminifera of oxygen-depleted environments, in: Modern foraminifera, Springer, 201–216, 1999.

Bernhard, J. M., Sen Gupta, B. K., and Borne, P. F.: Benthic foraminiferal proxy to estimate dysoxic bottom water oxygen concentration: Santa Barbara basin U.S. Pacific continental margin, J. Foramin. Res., 27, 301–310, 1997.

Bova, S. C., Herbert, T., Rosenthal, Y., Kalansky, J., Altabet, M., Chazen, C., Mojarro, A., and Zech, J.: Links between eastern equatorial Pacific stratification and atmospheric $CO_2$ rise during the last deglaciation, Paleoceanography, 30, 1407–1424, 2015.

Bova, S. C., Herbert, T. D., and Altabet, M. A.: Ventilation of northern and southern sources of aged carbon in the eastern equatorial Pacific during the Younger Dryas rise in atmospheric $CO_2$, Paleoceanogr. Paleocl., 33, 1151–1168, 2018.

Boyer, T. P., Antonov, J. I., Baranova, O. K., Coleman, C., Garcia, H. E., Grodsky, A., Johnson, D. R., Locarnini, R. A., Mishonov, A. V., O'Brien, T. D., Paver, C. R., Reagan, J. R., Seidov, D., Smolyar, I. V., and Zweng, M. M.: World Ocean Database 2013, NOAA Atlas NESDIS 72, edited by: Levitus, S., National Oceanographic Data Center Ocean Climate Laboratory, 208 pp., 2013.

Brandt, P., Bange, H. W., Banyte, D., Dengler, M., Didwischus, S.-H., Fischer, T., Greatbatch, R. J., Hahn, J., Kanzow, T., Karstensen, J., Körtzinger, A., Krahmann, G., Schmidtko, S.,

Stramma, L., Tanhua, T., and Visbeck, M.: On the role of circulation and mixing in the ventilation of oxygen minimum zones with a focus on the eastern tropical North Atlantic, Biogeosciences, 12, 489–512, https://doi.org/10.5194/bg-12-489-2015, 2015.

Cannariato, K. G. and Kennett, J. P.: Climatically related millenial-scale fluctuations in strength of California margin oxygen-minimum zone during the past 60 ky, Geology, 27, 975–978, 1999.

Cannariato, K. G., Kennett, J. P., and Behl, R. J.: Biotic response to late Quaternary rapid climate switches in Santa Barbara Basin: Ecological and evolutionary implications, Geology, 27, 63–66, 1999.

Caralp, M. H.: Abundance of *Bulimina exilis* and *Melonis barleeanum*: Relationship to the quality of marine organic matter, Geo-Mar. Lett., 9, 37–43, 1989.

Cardich, J., Morales, M., Quipúzcoa, L., Sifeddine, A., and Gutiérrez, D.: Benthic Foraminiferal Communities and Microhabitat Selection on the Continental Shelf Off Central Peru, in: Anoxia, Springer, Dordrecht, 323–340, https://doi.org/10.1007/978-94-007-1896-8_17, 2012.

Cardich, J., Gutiérrez, D., Romero, D., Pérez, A., Quipúzcoa, L., Marquina, R., Yupanqui, W., Solís, J., Carhuapoma, W., Sifeddine, A., and Rathburn, A.: Calcareous benthic foraminifera from the upper central Peruvian margin: control of the assemblage by pore water redox and sedimentary organic matter, Mar. Ecol. Prog. Ser., 535, 63–87, https://doi.org/10.3354/meps11409, 2015.

Cardich, J., Sifeddine, A., Salvatteci, R., Romero, D., Briceño-Zuluaga, F., Graco, M., Anculle, T., Almeida, C., and Gutiérrez, D.: Multidecadal changes in marine subsurface oxygenation off central Peru during the last ca. 170 years, Front. Mar. Sci., 6, 1–16, https://doi.org/10.3389/fmars.2019.00270, 2019.

Caulle, C., Koho, K. A., Mojtahid, M., Reichart, G. J., and Jorissen, F. J.: Live (Rose Bengal stained) foraminiferal faunas from the northern Arabian Sea: faunal succession within and below the OMZ, Biogeosciences, 11, 1155–1175, https://doi.org/10.5194/bg-11-1155-2014, 2014.

Chaigneau, A., Dominguez, N., Eldin, G., Vasquez, L., Flores, R., Grados, C., and Echevin, V.: Near-coastal circulation in the Northern Humboldt Current System from shipboard ADCP data, J. Geophys. Res.-Ocean., 118, 5251–5266, https://doi.org/10.1002/jgrc.20328, 2013.

Dale, A. W., Sommer, S., Lomnitz, U., Montes, I., Treude, T., Liebetrau, V., Gier, J., Hensen, C., Dengler, M., Stolpovsky, K., Bryant, L. D., and Wallmann, K.: Organic carbon production, mineralisation and preservation on the Peruvian margin, Biogeosciences, 12, 1537–1559, https://doi.org/10.5194/bg-12-1537-2015, 2015.

den Dulk, M., Reichart, G. J., Memon, G. M., Roelofs, E. M. P., Zachariasse, W. J., and van der Zwaan, G. J.: Benthic foraminiferal response to variations in surface water productivity and oxygenation in the northern Arabian Sea, Mar. Micropaleontol., 35, 43–66, 1998.

den Dulk, M., Reichart, G. J., van Heyst, S., Zachariasse, W. J., and Van der Zwaan, G. J.: Benthic foraminifera as proxies of organic matter flux and bottom water oxygenation? A case history from the Northern Arabian Sea, Palaeogeogr. Palaeocl., 161, 337–359, 2000.

Doering, K., Erdem, Z., Ehlert, C., Fleury, S., Frank, M., and Schneider, R.: Changes in diatom productivity and upwelling in-

tensity off Peru since the Last Glacial Maximum: Response to basin-scale atmospheric and oceanic forcing, Paleoceanography, 31, 1453–1473, https://doi.org/10.1002/2016pa002936, 2016.

Douglas, R. G. and Heitman, H. L.: Slope and basin benthic foraminifera of the California Borderland, Soc. Econ. Pa., 27, 231–246, 1979.

Erdem, Z. and Schönfeld, J.: Pleistocene to Holocene benthic foraminiferal assemblages from the Peruvian continental margin, Palaeontol. Electron., 20.2.35A, 1–32, https://doi.org/10.26879/764, 2017.

Erdem, Z., Schönfeld, J., Glock, N., Dengler, M., Mosch, T., Sommer, S., Elger, J., and Eisenhauer, A.: Peruvian sediments as recorders of an evolving hiatus for the last 22 thousand years, Quaternary Sci. Rev., 137, 1–14, https://doi.org/10.1016/j.quascirev.2016.01.029, 2016.

Erdem, Z., Schönfeld, J., Rathburn, A. E., Pérez, M. E., Cardich, J., and Glock, N.: Peruvian Margin living benthic foraminiferal distributions in percentage, PANGAEA, https://doi.org/10.1594/PANGAEA.901840, 2019.

Fontanier, C., Duros, P., Toyofuku, T., Oguri, K., Koho, K. A., Buscail, R., Grémare, A., Radakovitch, O., Deflandre, B., Nooijer, L. J. D., Bichon, S., Goubet, S., Ivanovsky, A., Chabaud, G., Menniti, C., Reichart, G.-J., and Kitazato, H.: Living (stained) deep-sea foraminifera off Hachinohe (NE Japan, western Pacific): environmental interplay in oxygen-depleted ecosystems, J. Foramin. Res., 44, 281–299, 2014.

Fuenzalida, R., Schneider, W., Garcés-Vargas, J., Bravo, L., and Lange, C.: Vertical and horizontal extension of the oxygen minimum zone in the eastern South Pacific Ocean, Deep-Sea Res. Pt. II, 56, 992–1003, 2009.

Geslin, E., Heinz, P., Jorissen, F., and Hemleben, C.: Migratory responses of deep-sea benthic foraminifera to variable oxygen conditions: laboratory investigations, Mar. Micropaleontol., 53, 227–243, https://doi.org/10.1016/j.marmicro.2004.05.010, 2004.

Glock, N., Eisenhauer, A., Milker, Y., Liebetrau, V., Schönfeld, J., Mallon, J., Sommer, S., and Hensen, C.: Environmental influences on the pore density of Bolivina spissa (Cushman), J. Foramin. Res., 41, 22–32, 2011.

Glock, N., Erdem, Z., Wallmann, K., Somes, C. J., Liebetrau, V., Schonfeld, J., Gorb, S., and Eisenhauer, A.: Coupling of oceanic carbon and nitrogen facilitates spatially resolved quantitative reconstruction of nitrate inventories, Nat. Commun., 9, 1217, https://doi.org/10.1038/s41467-018-03647-5, 2018.

Glock, N., Roy, A.-S., Romero, D., Wein, T., Weissenbach, J., Revsbech, N. P., Høgslund, S., Clemens, D., Sommer, S., and Dagan, T.: Metabolic preference of nitrate over oxygen as an electron acceptor in foraminifera from the Peruvian oxygen minimum zone, P. Natl. Acad. Sci. USA, 116, 2860–2865, 2019.

Glud, R. N., Thamdrup, B., Stahl, H., Wenzhoefer, F., Glud, A., Nomaki, H., Oguri, K., Revsbech, N. P., and Kitazato, H.: Nitrogen cycling in a deep ocean margin sediment (Sagami Bay, Japan), Limnol. Oceanogr., 54, 723–734, 2009.

Golik, A. and Phleger, F. B.: Benthonic foraminifera from the Gulf of Panama, J. Foramin. Res., 7, 83–99, 1977.

Gonzales, M. V., De Almeida, F. K., Costa, K. B., Santarosa, A. C. A., Camillo Jr, E., De Quadros, J. P., and Toledo, F. A.: HelP index: Hoeglundina elegans preservation index for marine sediments in the western South Atlantic, J. Foramin. Res., 47, 56–69, 2017.

Gooday, A. J.: A response by benthic Foraminifera to the deposition of phytodetritus in the deep sea, Nature, 332, 70–73, https://doi.org/10.1038/332070a0, 1988.

Gooday, A. J.: Deep-sea benthic foraminiferal species which exploit phytodetritus: characteristic features and controls on distribution, Mar. Micropaleontol., 22, 187–205, 1993.

Gooday, A. J.: Benthic foraminifera (Protista) as tools in deep-water palaeoceanography: environmental influences on faunal characteristics, Adv. Mar. Biol., 46, 1–90, https://doi.org/10.1016/S0065-2881(03)46002-1, 2003.

Gooday, A. J. and Jorissen, F. J.: Benthic foraminiferal biogeography: controls on global distribution patterns in deep-water settings, Ann. Rev. Mar. Sci., 4, 237–262, https://doi.org/10.1146/annurev-marine-120709-142737, 2012.

Gooday, A. J. and Rathburn, A. E.: Temporal variability in living deep-sea benthic foraminifera: a review, Earth-Sci. Rev., 46, 187–212, 1999.

Gooday, A. J., Bernhard, J. M., Levin, L. A., and Suhr, S. B.: Foraminifera in the Arabian Sea oxygen minimum zone and other oxygen-deficient settings: taxonomic composition, diversity, and relation to metazoan faunas, Deep-Sea Res. Pt. II, 47, 25–54, 2000.

Gupta, A. K. and Thomas, E.: Initiation of Northern Hemisphere glaciation and strengthening of the northeast Indian monsoon: Ocean Drilling Program Site 758, eastern equatorial Indian Ocean, Geology, 31, 47–50, 2003.

Hammer, Ø., Harper, D., and Ryan, P.: PAST-Palaeontological statistics, available at: http://www.uv.es/~pardomv/pe/2001_1/past/pastprog/past.pdf (last access: 12 June 2020), 2001.

Heinze, P.-M. and Wefer, G.: The history of coastal upwelling off Peru (11° S, ODP Leg 112, Site 680B) over the past 650 000 years, Geol. Soc. Lond. Special Publ., 64, 451–462, 1992.

Helly, J. J. and Levin, L. A.: Global distribution of naturally occurring marine hypoxia on continental margins, Deep-Sea Res. Pt. I, 51, 1159–1168, 2004.

Hendy, I. L. and Pedersen, T. F.: Oxygen minimum zone expansion in the eastern tropical North Pacific during deglaciation, Geophys. Res. Lett., 33, L20602, https://doi.org/10.1029/2006GL025975, 2006.

Hermelin, J. O. R. and Shimmield, G. B.: The importance of the oxygen minimum zone and sediment geochemistry in the distribution of Recent benthic foraminifera in the northwest Indian Ocean, Mar. Geol., 91, 1–29, 1990.

Hoogakker, B. A. A., Lu, Z., Umling, N., Jones, L., Zhou, X., Rickaby, R. E. M., Thunell, R., Cartapanis, O., and Galbraith, E.: Glacial expansion of oxygen-depleted seawater in the eastern tropical Pacific, Nature, 562, 410–413, https://doi.org/10.1038/s41586-018-0589-x, 2018.

Ingle, J. C., Keller, G., and Kolpack, R. L.: Benthic foraminiferal biofacies, sediments and water masses of the southern Peru-Chile Trench area, southeastern Pacific Ocean, Micropaleontology, 26, 113–150, 1980.

Jaccard, S. L. and Galbraith, E. D.: Large climate-driven changes of oceanic oxygen concentrations during the last deglaciation, Nat. Geosci., 5, 151–156, 2012.

Jaccard, S. L., Galbraith, E. D., Frölicher, T. L., and Gruber, N.: Ocean (de) oxygenation across the last deglaciation: Insights for the future, Oceanography, 27, 26–35, 2014.

Jannink, N. T., Zachariasse, W. J., and van der Zwaan, G. J.: Living (Rose Bengal stained) benthic foraminifera from the Pakistan continental margin (northern Arabian Sea), Deep-Sea Res. Pt. I, 45, 1483–1513, 1998.

Jorissen, F. J., de Stigter, H. C., and Widmark, J. G.: A conceptual model explaining benthic foraminiferal microhabitats, Mar. Micropaleontol., 26, 3–15, 1995.

Kaiho, K.: Benthic foraminiferal dissolved-oxygen index and dissolved-oxygen levels in the modern ocean, Geology, 22, 719–722, https://doi.org/10.1130/0091-7613(1994)022<0719:bfdoia>2.3.co;2, 1994.

Karstensen, J., Stramma, L., and Visbeck, M.: Oxygen minimum zones in the eastern tropical Atlantic and Pacific oceans, Prog. Oceanogr., 77, 331–350, 2008.

Khusid, T. A.: Distribution of benthic foraminifers off west coast of South America, Oceanology-USSR, 14, 900–904, 1974.

Kuhnt, T., Friedrich, O., Schmiedl, G., Milker, Y., Mackensen, A., and Lückge, A.: Relationship between pore density in benthic foraminifera and bottom-water oxygen content, Deep-Sea Res. Pt. I, 76, 85–95, 2013.

Leiter, C. and Altenbach, A. V.: Benthic foraminifera from the diatomaceous mud belt off Namibia: Characteristic species for severe anoxia, Palaeontol. Electron., 13.2.11A, 2010.

Levin, L.: Oxygen minimum zone benthos: adaptation and community response to hypoxia, in: Oceanogr. Marine Biol. Annu. Rev., edited by: Gibson, R. and Atkinson, R., Taylor&Francis, London, 1–45, 2003.

Levin, L., Gutiérrez, D., Rathburn, A., Neira, C., Sellanes, J., Muñoz, P., Gallardo, V., and Salamanca, M.: Benthic processes on the peru margin: a transect across the oxygen minimum zone during the 1997–98 El Niño, Prog. Oceanogr., 53, 1–27, 2002.

Levin, L. A.: Manifestation, drivers, and emergence of open ocean deoxygenation, Ann. Rev. Mar. Sci., 10, 229–260, 2018.

Loubere, P.: A multiproxy reconstruction of biological productivity and oceanography in the eastern equatorial Pacific for the past 30,000 years, Mar. Micropaleontol., 37, 173–198, 1999.

Mackensen, A. and Douglas, R. G.: Down-core distribution of live and dead deep-water benthic foraminifera in box cores from the Weddell Sea and the California continental borderland, Deep-Sea Res. Pt. A, 36, 879–900, 1989.

Mackensen, A., Grobe, H., Kuhn, G., and Fütterer, D. K.: Benthic foraminiferal assemblages from the eastern Weddell Sea between 68 and 73° S: Distribution, ecology and fossilization potential, Mar. Micropaleontol., 16, 241–283, 1990.

Mallon, J.: Benthic foraminifera of the Peruvian and Ecuadorian continental margin, PhD Dissertation, Christian-Albrechts-Universität zu Kiel, 236 pp., 2012.

Mallon, J., Glock, N., and Schönfeld, J.: The response of benthic foraminifera to low-oxygen conditions of the Peruvian oxygen minimum zone, in: Anoxia, Springer, Dordrecht, 305–321, 2012.

Martin, J. H., Knauer, G. A., Karl, D. M., and Broenkow, W. W.: VERTEX: carbon cycling in the northeast Pacific, Deep-Sea Res. Pt. A, 34, 267–285, 1987.

Martinez, P. and Robinson, R. S.: Increase in water column denitrification during the last deglaciation: the influence of oxygen demand in the eastern equatorial Pacific, Biogeosciences, 7, 1–9, https://doi.org/10.5194/bg-7-1-2010, 2010.

McKay, C. L., Groeneveld, J., Filipsson, H. L., Gallego-Torres, D., Whitehouse, M. J., Toyofuku, T., and Romero, O. E.: A compar-

ison of benthic foraminiferal Mn/Ca and sedimentary Mn/Al as proxies of relative bottom-water oxygenation in the low-latitude NE Atlantic upwelling system, Biogeosciences, 12, 5415–5428, https://doi.org/10.5194/bg-12-5415-2015, 2015.

Members, E. C., Barbante, C., Barnola, J.-M., Becagli, S., Beer, J., Bigler, M., Boutron, C., Blunier, T., Castellano, E., and Cattani, O.: One-to-one coupling of glacial climate variability in Greenland and Antarctica, Nature, 444, 195–198, 2006.

Moffitt, S. E., Hill, T. M., Ohkushi, K., Kennett, J. P., and Behl, R. J.: Vertical oxygen minimum zone oscillations since 20 ka in Santa Barbara Basin: A benthic foraminiferal community perspective, Paleoceanography, 29, 44–57, 2014.

Moffitt, S. E., Moffitt, R. A., Sauthoff, W., Davis, C. V., Hewett, K., and Hill, T. M.: Paleoceanographic insights on recent oxygen minimum zone expansion: Lessons for modern oceanography, PloS One, 10, e0115246, https://doi.org/10.1371/journal.pone.0115246, 2015.

Mollier-Vogel, E., Leduc, G., Böschen, T., Martinez, P., and Schneider, R. R.: Rainfall response to orbital and millennial forcing in northern Peru over the last 18 ka, Quaternary Sci. Rev., 76, 29–38, https://doi.org/10.1016/j.quascirev.2013.06.021, 2013.

Mollier-Vogel, E., Martinez, P., Blanz, T., Robinson, R., Desprat, S., Etourneau, J., Charlier, K., and Schneider, R. R.: Mid-Holocene deepening of the Southeast Pacific oxycline, Glob. Planet. Change, 172, 365–373, 2019.

Montes, I., Colas, F., Capet, X., and Schneider, W.: On the pathways of the equatorial subsurface currents in the eastern equatorial Pacific and their contributions to the Peru-Chile Undercurrent, J. Geophys. Res.-Ocean., 115, C09003, https://doi.org/10.1029/2009JC005710, 2010.

Mullins, H. T., Thompson, J. B., McDougall, K., and Vercoutere, T. L.: Oxygen-minimum zone edge effects: evidence from the central California coastal upwelling system, Geology, 13, 491–494, 1985.

Murray, J. W.: Ecology and applications of benthic foraminifera, Cambridge University Press, 426 pp., 2006.

Nomaki, H., Heinz, P., Nakatsuka, T., Shimanaga, M., Ohkouchi, N., Ogawa, N. O., Kogure, K., Ikemoto, E., and Kitazato, H.: Different ingestion patterns of $^{13}$C-labeled bacteria and algae by deep-sea benthic foraminifera, Mar. Ecol. Prog. Ser., 310, 95–108, 2006.

Nordberg, K., Gustafsson, M., and Krantz, A.-L.: Decreasing oxygen concentrations in the Gullmar Fjord, Sweden, as confirmed by benthic foraminifera, and the possible association with NAO, J. Mar. Syst., 23, 303–316, 2000.

Oberhänsli, H., Heinze, P., Diester-Haass, L., and Wefer, G.: Upwelling off Peru during the last 430,000 yr and its relationship to the bottom-water environment, as deduced from coarse grain-size distributions and analyses of benthic foraminfers at holes 679D, 680B, and 681B, Leg 112, in: Proceedings of the Ocean Drilling Program: Scientific results, edited by: Suess, E., von Huene, R. et al., IODP, 369–390, 1990.

Ohga, T. and Kitazato, H.: Seasonal changes in bathyal foraminiferal populations in response to the flux of organic matter (Sagami Bay, Japan), Terra Nova, 9, 33–37, 1997.

Oschlies, A., Brandt, P., Stramma, L., and Schmidtko, S.: Drivers and mechanisms of ocean deoxygenation, Nat. Geosci., 11, 467–473, 2018.

Paulmier, A. and Ruiz-Pino, D.: Oxygen minimum zones (OMZs) in the modern ocean, Prog. Oceanogr., 80, 113–128, 2009.

Pedersen, T. F.: Increased productivity in the eastern equatorial Pacific during the last glacial maximum (19,000 to 14,000 yr B.P.), Geology, 11, 16–19, https://doi.org/10.1130/0091-7613(1983)11<16:ipitee>2.0.co;2, 1983.

Pedersen, T. F., Pickering, M., Vogel, J. S., Southon, J. N., and Nelson, D. E.: The response of benthic foraminifera to productivity cycles in the eastern equatorial Pacific: Faunal and geochemical constraints on glacial bottom water oxygen levels, Paleoceanography, 3, 157–168, 1988.

Pennington, J. T., Mahoney, K. L., Kuwahara, V. S., Kolber, D. D., Calienes, R., and Chavez, F. P.: Primary production in the eastern tropical Pacific: A review, Prog. Oceanogr., 69, 285–317, 2006.

Phleger, F. B. and Soutar, A.: Production of benthic foraminifera in three east Pacific oxygen minima, Micropaleontology, 19, 110–115, 1973.

Piña-Ochoa, E., Høgslund, S., Geslin, E., Cedhagen, T., Revsbech, N. P., Nielsen, L. P., Schweizer, M., Jorissen, F., Rysgaard, S., and Risgaard-Petersen, N.: Widespread occurrence of nitrate storage and denitrification among Foraminifera and Gromiida, P. Natl. Acad. Sci. USA, 107, 1148–1153, 2010.

Praetorius, S. K., Mix, A. C., Walczak, M., Wolhowe, M. D., Addison, J. A., and Prahl, F. G.: North Pacific deglacial hypoxic events linked to abrupt ocean warming, Nature, 527, 362–366, 2015.

Rathburn, A. E., Willingham, J., Ziebis, W., Burkett, A. M., and Corliss, B. H.: A New biological proxy for deep-sea paleo-oxygen: Pores of epifaunal benthic foraminifera, Sci. Rep., 8, 9456, https://doi.org/10.1038/s41598-018-27793-4, 2018.

Reimer, P. J., Bard, E., Bayliss, A., Beck, J. W., Blackwell, P. G., Ramsey, C. B., Buck, C. E., Cheng, H., Edwards, R. L., and Friedrich, M.: IntCal13 and Marine13 radiocarbon age calibration curves 0–50,000 years cal BP, Radiocarbon, 55, 1869–1887, 2013.

Reimers, C. E. and Suess, E.: Spatial and temporal patterns of organic matter accumulation on the Peru continental margin, in: Coastal upwelling, its sediment record, Part B: sedimentary records of ancient coastal upwelling, edited by: Thiede, J. and Suess, E., NATO Conference Series IV: Marine Sciences, 10b, Plenum Press, New York, 311–345, 1983.

Resig, J. M.: Biogeography of benthic foraminifera of the northern Nazca plate and adjacent continental margin, Geol. Soc. Am. Mem., 154, 619–644, 1981.

Resig, J. M.: Benthic foraminiferal stratigraphy and paleoenvironments off Peru leg 112, in: Proceedings of the Ocean Drilling Program, Scientific Results, edited by: Suess, E., Von Huene, R. et al., Ocean Drilling Program, College Station, TX, 263–296, 1990.

Salvatteci, R., Gutiérrez, D., Sifeddine, A., Ortlieb, L., Druffel, E., Boussafir, M., and Schneider, R.: Centennial to millennial-scale changes in oxygenation and productivity in the Eastern Tropical South Pacific during the last 25,000 years, Quaternary Sci. Rev., 131, 102–117, 2016.

Salvatteci, R., Schneider, R., Blanz, T., and Mollier-Vogel, E.: Deglacial to Holocene Ocean Temperatures in the Humboldt Current System as Indicated by Alkenone Paleothermometry, Geophys. Res. Lett., 46, 281–292, 2018.

Sarkar, S. and Gupta, A. K.: Late Quaternary productivity changes in the equatorial Indian Ocean (ODP Hole 716A), Palaeogeogr. Palaeocl., 397, 7–19, 2014.

Sarnthein, M., Küssner, K., Grootes, P. M., Ausin, B., Eglinton, T., Muglia, J., Muscheler, R., and Schlolaut, G.: Plateaus and jumps in the atmospheric radiocarbon record – Potential origin and value as global age markers for glacial-to-deglacial paleoceanography, a synthesis, Clim. Past Discuss., https://doi.org/10.5194/cp-2019-127, in review, 2019.

Schmidtko, S., Stramma, L., and Visbeck, M.: Decline in global oceanic oxygen content during the past five decades, Nature, 542, 335–339, 2017.

Schmiedl, G., Mackensen, A., and Müller, P.: Recent benthic foraminifera from the eastern South Atlantic Ocean: dependence on food supply and water masses, Mar. Micropaleontol., 32, 249–287, 1997.

Schmiedl, G., Mitschele, A., Beck, S., Emeis, K.-C., Hemleben, C., Schulz, H., Sperling, M., and Weldeab, S.: Benthic foraminiferal record of ecosystem variability in the eastern Mediterranean Sea during times of sapropel $S_5$ and $S_6$ deposition, Palaeogeogr. Palaeocl., 190, 139–164, 2003.

Scholz, F., McManus, J., Mix, A. C., Hensen, C., and Schneider, R. R.: The impact of ocean deoxygenation on iron release from continental margin sediments, Nat. Geosci., 7, 433–437, 2014.

Schönfeld, J. and Altenbach, A. V.: Late Glacial to Recent distribution pattern of deep-water Uvigerina species in the north-eastern Atlantic, Mar. Micropaleontol., 57, 1–24, https://doi.org/10.1016/j.marmicro.2005.05.004, 2005.

Schönfeld, J., Kuhnt, W., Erdem, Z., Flögel, S., Glock, N., Aquit, M., Frank, M., and Holbourn, A.: Records of past mid-depth ventilation: Cretaceous ocean anoxic event 2 vs. Recent oxygen minimum zones, Biogeosciences, 12, 1169–1189, https://doi.org/10.5194/bg-12-1169-2015, 2015.

Schröder, C. J.: Subsurface Preservation of Agglutinated Foraminifera in the Northwest Atlantic Ocean, Abh. Geol. B.-A., 41, 325–336, 1988.

Schumacher, S., Jorissen, F. J., Dissard, D., Larkin, K. E., and Gooday, A. J.: Live (Rose Bengal stained) and dead benthic foraminifera from the oxygen minimum zone of the Pakistan continental margin (Arabian Sea), Mar. Micropaleontol., 62, 45–73, 2007.

Sen Gupta, B. K. and Machain-Castillo, M. L.: Benthic foraminifera in oxygen-poor habitats, Mar. Micropaleontol., 20, 183–201, 1993.

Siani, G., Michel, E., De Pol-Holz, R., Devries, T., Lamy, F., Carel, M., Isguder, G., Dewilde, F. and Lourantou, A.: Carbon isotope records reveal precise timing of enhanced Southern Ocean upwelling during the last deglaciation, Nat. Commun., 4, 1–9, https://doi.org/10.1038/ncomms3758, 2013.

Smart, C. W., King, S. C., Gooday, A. J., Murray, J. W., and Thomas, E.: A benthic foraminiferal proxy of pulsed organic matter paleofluxes, Mar. Micropaleontol., 23, 89–99, 1994.

Smith, P. B.: Ecology of benthonic species, Recent foraminifera off Central America, Geological Survey Professional Paper, Washington, 53 pp., 1964.

Sommer, S.: Short Cruise Report RV *METEOR* M137 Callao (Peru) – Callao (Peru) 06.05.2017–29.05.2017, Project: Collaborative Research Centre 754 "Climate – Biogeochemistry Interactions in the Tropical Ocean", 1–13, 2017.

Stern, J. V. and Lisiecki, L. E.: Termination 1 timing in radiocarbon-dated regional benthic $\delta^{18}$O stacks, Paleoceanography, 29, 1127–1142, 2014.

Stramma, L., Johnson, G. C., Sprintall, J., and Mohrholz, V.: Expanding oxygen-minimum zones in the tropical oceans, Science, 320, 655–658, 2008.

Tetard, M., Licari, L., and Beaufort, L.: Oxygen history off Baja California over the last 80 kyr: A new foraminiferal-based record, Paleoceanography, 32, 246–264, 2017.

Tyson, R. V. and Pearson, T. H.: Modern and ancient continental shelf anoxia: an overview, Geol. Soc. Lond. Special Publ., 58, 1–24, 1991.

Uchio, T.: Ecology of living benthonic Foraminifera frpm the San Diego, California area, Cushman Foundation Foraminifera Research Special Publications, 5, 1–72, 1960.

Van der Zwaan, G. J.: Benthic foraminifers proxies or problems? A review of paleoecological concepts, Earth-Sci. Rev., 46, 213–236, 1999.

Venturelli, R. A., Rathbun, A. E., Burkett, A. M., and Ziebis, W.: Epifaunal foraminifera in an infaunal world: insights into the influence of heterogeneity on the benthic ecology of oxygen-poor, deep-sea habitats, Front. Mar. Sci., 5, 1–13, https://doi.org/10.3389/fmars.2018.00344, 2018.

Wyrtki, K.: The oxygen minima in relation to ocean circulation, in: Deep Sea Research and Oceanographic Abstracts, Elsevier, 9, 11–23, 1962.

Yamamoto, A., Abe-Ouchi, A., Ohgaito, R., Ito, A., and Oka, A.: Glacial $CO_2$ decrease and deep-water deoxygenation by iron fertilization from glaciogenic dust, Clim. Past, 15, 981–996, https://doi.org/10.5194/cp-15-981-2019, 2019.

Zhao, N. and Keigwin, L. D.: An atmospheric chronology for the glacial-deglacial Eastern Equatorial Pacific, Nat. Commun., 9, 3077, https://doi.org/10.1038/s41467-018-05574-x, 2018.